文章编号：1000-0550(2024)00-0000-00　　DOI：10.14027/j.issn.1000-0550.2024.135

细粒沉积岩物质来源及成因研究现状

刘旭东，彭军，许天宇，王豪楠

“天然气地质”四川省重点实验室，西南石油大学地球科学与技术学院，成都 610500

摘 要 【意义】细粒沉积岩物质来源研究作为细粒沉积岩“源—汇”系统理论中的首要环节，对恢复古环境、理解细粒沉积岩形成机理和预测非常规油气资源等方面有着重要意义。细粒沉积岩具有物质组成粒度较小、成分复杂、观察研究难度大的特点，且不同物质成分对应多样的物质来源和成因。纵观国内外现有的研究成果，目前仍旧缺乏针对细粒沉积物质来源及成因研究成果的系统性梳理和归纳总结。【进展】综合当前研究成果，将细粒沉积岩的物质来源归纳为陆源、内源和火山—热液源三大类。对常见细粒沉积物来源及成因进行了深入的归纳和总结，指出：（1）黏土矿物为陆源物质风化成因、成岩作用阶段其他矿物转化成因和黏土矿物之间转化成因、海底火山物质海解成因以及胞外聚合物生物介导作用成因；（2）石英主要源于陆源物质风化、盆内生物作用、火山凝灰物质脱玻化作用以及成岩作用；（3）长石源于陆源碎屑物质风化，火山—热液作用输入，近年来相关研究也发现长石能够由微生物化学作用形成；（4）碳酸盐矿物主要是内源物质，其能够由在盆内由化学作用、生物—化学作用、生物作用和搬运再沉积作用形成，另外陆源物质和火山—热液源物质的输入不仅能直接为细粒沉积岩提供碳酸盐矿物也会促使盆内碳酸盐矿物的形成；（5）黄铁矿主要由铁和硫两大成矿元素在盆内分别经过异化铁还原作用和铁穿梭机制主导还原作用、微生物还原作用和硫酸盐热化学还原作用形成；（6）有机质可划分为陆源的镜质体、惰质体和部分类脂体以及内源的部分类脂体、动物有机碎屑和次生有机质。【展望与结论】未来细粒沉积岩物质来源及成因的研究将围绕多学科、高精度等方面发展，当下仍亟待一套适用于细粒沉积岩物源研究的系统方案形成。细粒沉积岩物质来源和物质成因的系统性梳理与总结，增进了对细粒沉积物质来源和形成机制的理解，从而推动细粒沉积学理论的发展，为明确细粒沉积地层的展布特征、预测非常规油气资源的分布提供坚实的理论基础和科学依据。

关键词 细粒沉积岩；物质来源；物质特征；成因机制

第一作者简介 刘旭东，男，1999 年出生，硕士研究生，细粒沉积学，E-mail:15339127783@163.com

通信作者 彭军，男，教授，博士生导师，沉积学、层序地层学与储层地质学，E-mail：445371976@qq.com

中图分类号 P512.2 P618.13 **文献标志码** A

0 引言

在全球能源消费结构转型的背景下，美国“页岩革命”取得了显著成就，从常规油气向非常规油气过渡已然成为全球石油工业的发展趋势[1-2]。细粒沉积岩作为非常规油气资源重要的烃源岩和储集层，近年来在石油地质学领域的研究热度如日中天。细粒沉积岩是指粒级小于 62.5μm、含量大于 50%的组分构成的沉积岩类[3]。与碎屑岩、碳酸盐岩相比，细粒沉积岩具有粒度较小、物质成分复杂、观察研究难度大的特点，因此其在物质来源、搬运—沉

收稿日期：2024-08-19；**收修改稿日期**：2024-12-27
基金项目：国家自然科学基金面上项目（41872166）[**Foundation:** National Natural Science Foundation of China, No. 41872166]

积机制、成岩作用乃至沉积环境、沉积相划分等方面的研究程度均远远落后于碎屑岩、碳酸盐岩的研究[4-5]。

黏土矿物、石英、长石、碳酸盐矿物、黄铁矿、有机质等是细粒沉积岩中常见的物质成分[4]。如此复杂的物质组成，难以避免其物源及物质成因的多样性和复杂性，例如细粒沉积岩中的碳酸盐矿物，不仅可以由盆内的物理—化学作用、生物—化学作用、生物作用形成细粒级别的碳酸盐矿物[6-7]，也可以由陆源区白云岩、大理岩等碳酸盐矿物含量较高的岩石经过一系列地质作用形成[8]，还能由水底热液直接向盆内输入细粒级别的碳酸盐矿物[9-11]。

物质来源作为细粒沉积岩研究中的重要课题之一，对于发展和完善细粒沉积岩的相关基础理论有着不可忽视的意义，如：提供古地理、古气候、古环境重建等重要信息以帮助了解细粒沉积岩的形成过程[12-14]。纵观国内外现有的研究成果，目前仍旧缺乏针对细粒沉积物质来源及物质成因相关研究成果的系统性梳理以及归纳总结。因此，本文基于前人对细粒沉积岩相关的认识成果，系统总结近年来其物质来源的研究现状，理清陆源、内源、火山—热液源物质相关特征，总结黏土矿物、石英、长石、碳酸盐矿物、黄铁矿、有机质等细粒沉积岩常见物质组成特征及其来源，指出目前存在的问题以及未来细粒沉积岩物质来源研究的发展趋势，供广大学者探讨。

1 细粒沉积岩物质来源

1.1 陆源

陆源细粒沉积物质几乎在所有细粒沉积岩中均有记录，这类沉积物质是指由陆源区母岩经过物理、化学、生物化学等风化作用形成的风化产物，经过河流、大气、冰川、生物等搬运介质搬运，并在搬运过程中进一步风化，最终沉积到盆地中形成的细粒沉积物质[15]。通常陆相湖盆中的陆源细粒沉积物质主要来源于河流以及冲积扇的输入，陆源区的火成岩、变质岩、沉积岩都能够作为细粒沉积岩的母岩，其陆源物质输入量不仅受控于陆源区的风化剥蚀、供源数量和搬运距离，还受到气候条件和水体状态的影响，此外陆源细粒沉积岩对陆源物质的输入的反应往往比海相细粒沉积岩更加强烈，物质组成、结构、构造与海相细粒沉积岩相比也更加复杂[16-18]。

陆源物质成分复杂，常见的有黏土矿物、石英、长石、碳酸盐矿物、有机质和多种化学元素。其中，陆源黏土矿物是源区母岩经过风化、淋滤作用释放出硅、铝等元素形成的产物[19]。陆源碎屑石英常呈次圆状—棱角状、粒级介于 10~50 μm 分布于细粒沉积岩中，通常风力搬运的陆源碎屑石英表面可见碟形撞击坑、新月形撞击坑、麻点；流水搬运的石英表面可

见水下磨光面、直线或弯曲状撞击沟、V 形撞击坑[20-23]。陆源碳酸盐矿物常由构造活动较强、气候较干旱、富含碳酸盐矿物的近物源区输入，通常分选和磨圆程度较低[24-26]。有机质中的镜质体、惰质体以及类脂体中的孢子体、角质体、树脂体等均是常见的陆源有机质[27-28]。此外，陆源也能向盆内输入大量的元素，为盆内物质的形成提供必要的物质基础。

1.2 内源

盆内来源的细粒沉积物质统称为内源细粒沉积物质，这类细粒沉积物是由湖或海盆内物理—化学作用、生物—化学作用以及生物作用沉积下来的细粒物质[29-30]。尽管目前对于细粒碳酸盐岩的物质来源和成因缺乏系统研究，但依旧可以明确内源仍然是其稳定来源[29]。常见的内源细粒沉积物除了碳酸盐矿物外，石英、Al、Fe、Mn 的氧化物以及氢氧化物、硫酸盐、有机质等也均是内源的常见物质[31]。另外，陆源物质输入、火山—热液活动与内源细粒物质来源关系密切[32]：陆源的石灰岩、白云岩、大理岩、玄武岩、碳酸岩等岩石经过风化淋滤作用向湖盆内输入 Ca^{2+}、Mg^{2+}等成分，为内源细粒物质形成提供必备条件[8,33]；火山活动形成的火山物质为湖盆内提供 Ca^{2+}、Al^{3+}、Fe^{3+}、Mg^{2+}等成分，在一定程度上促进内源细粒沉积物质的生成[34]。

内源细粒沉积物按成因可分为盆内化学物质、生物源物质和再搬运沉积物质[35]。盆内化学物质形成主要有化学作用和生物化学作用：化学物质是指盆内离子在高盐度、较高温度、较大 CO_2 分压环境下，直接从水体中析出并沉积的矿物类型，如江汉盆地潜江组页岩中大量的石盐和白云石等矿物均是化学作用成因[36]；生物化学作用是指通过生物生长活动改变沉积环境从而促进盆内矿物生成的作用，Dittrich *et al*.[37]发现湖泊中的细菌和藻类能够促进水体中的 Ca^{2+}和 CO_3^{2-}聚集，诱导方解石沉淀；此外 Liang *et al*.[34]对我国济阳坳陷古近系页岩中碳酸盐矿物进行研究也认为碳酸盐矿物形成的关键机制是生物诱导的化学沉淀。生物源物质是生物作用直接形成的细粒沉积物，例如放射虫、海绵骨针、硅藻等对水体中的 SiO_2 分解、吸收形成生物机体，待死亡后 SiO_2 再次从生物机体内移出沉淀形成新的硅质矿物[38-40]；另外，盆内蓝绿藻、硅藻、微藻、浮游沟鞭藻等可以形成有机质。值得注意的是，陆源也能向盆内输入各种动植物碎屑，其也属于生物源物质但并非内源物质，由于陆源生物源物质除了有机质外，其他陆源生物源物质含量相较于内源生物源物质相比含量非常少，因此文章将除了陆源有机质以外的陆源生物源物质不做探讨。再搬运沉积物质是指盆内已经形成的沉积物质经过水动力作用破碎后重新沉积形成的沉积物质，如碳酸盐质的内碎屑。

1.3 火山—热液源

火山—热液活动可形成水体外喷发的火山碎屑和通过断层、热液喷口输送到湖泊或海洋

的热液沉积物[41-42]。近年来我国多个陆相含油气盆地内均发现主力烃源岩展布与火山—热液活动具有较好的耦合关系[41,43]，这与火山—热液活动向盆内输入大量主、微量元素促进有机质勃发息息相关[44-45]。但也有学者认为火山碎屑物质进入水体释放大量 Cu、Zn、HCl 等有害物质导致生物大量死亡，不利于有机质发育[46]。

火山碎屑物质的搬运、沉积机制与陆源碎屑物质相似：风力搬运、碎屑流、重力流、异重流等流体都能将火山碎屑物质搬运至盆地沉积。李森等[47]在对鄂尔多斯盆地长 7 段细粒沉积岩研究时发现中酸性火山灰喷发带来的火山晶屑形成的凝灰质层（图 1a~d），石英、长石晶形程度较好、无明显搬运特征，整体呈层状正粒序构造，指示火山碎屑物质由风力作用搬运至湖盆内悬浮沉积的特征。

热液沉积物质按照形成方式可分为喷流式沉积物与喷爆式沉积物，当产出粒度小于 62.5 μm 时可归纳为细粒沉积物的范畴[48-52]。喷流式沉积物是指热液进入水底经过沉积作用形成的沉积物[48,53]，按照矿物组成可分为以硅酸盐、硅铝酸盐、碳酸盐矿物为主的“白烟囱”型和以黄铜矿、黄铁矿、方铅矿、闪锌矿等为主的“黑烟囱”型[54-55]。我国在准噶尔盆地[56-57]、三塘湖盆地[58-59]、鄂尔多斯盆地[60-61]等盆地均发现含有喷流式沉积物的细粒沉积岩，且都以具有正粒序层理的纹层状、条带状构造的“白烟囱”型为主（图 1e~g）[58-62]。喷爆式沉积物是指固、液、气三相共存的深源岩浆、热液物质通过湖（海）底的喷流通道上升并喷发时，由于温度和压力的突然变化，导致深源岩浆和热液物质剧烈喷发所形成的细粒沉积物类型。在这个过程中，原先形成的岩浆矿物会发生爆炸性破碎，形成微小的晶体碎片，这些微粒晶体矿物碎屑随后与水体混合并沉积下来，形成细粒沉积岩的组成部分[50]。李哲萱等[63]在研究准噶尔盆地吉木萨尔凹陷芦草沟组黑色细粒沉积岩，发现其中发育一定量“斑状”方解石颗粒纹层，符合喷爆式沉积物的特性（图 1h~j）。

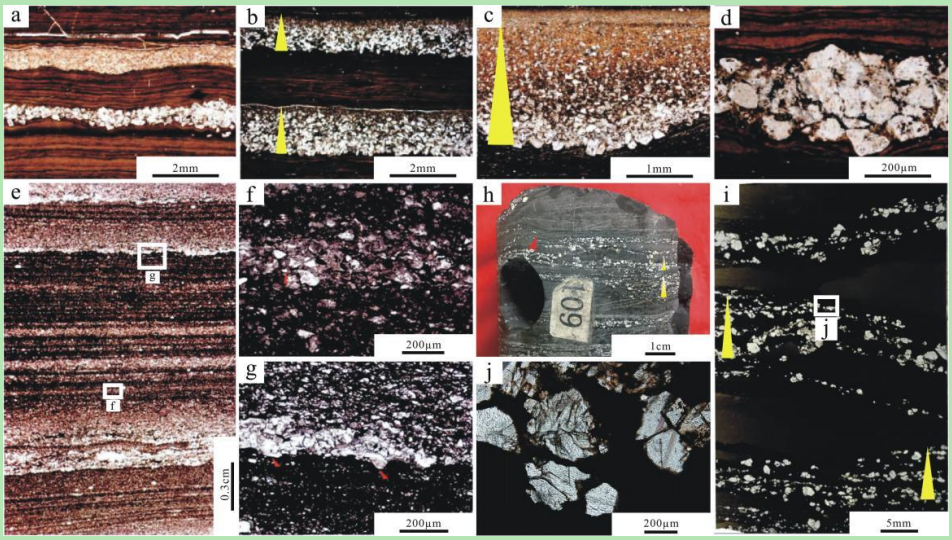

图 1　火山—热液源沉积物特征图

（a）水平纹层状页岩发育两期凝灰质层，下层为长英质晶屑火山灰层，上层为玻屑火山灰层，鄂尔多斯盆地长 7 段，YY1 井，228.44 m，单偏光[47]；（b）水平纹层状页岩发育两期正粒序火山晶屑，鄂尔多斯盆地长 7 段，YY1 井，229.60 m，单偏光[47]；（c）正粒序火山晶屑，鄂尔多斯盆地长 7 段，YY1 井，236.50 m，单偏光[47]；（d）图 a 中下层晶屑火山灰，鄂尔多斯盆地长 7 段，YY1 井，228.44 m，单偏光[47]；（e）纹层状火山碎屑（白色）岩与白云岩（深褐色）互层，三塘湖盆地芦草沟组，M11 井，2 944.80 m，单偏光[58]；（f）为 e 中 f 框的放大，长英质颗粒（白色）呈棱角状，个别具鸡骨状结构（红箭头）[58]；（g）为 e 中 g 框的放大，火山碎屑岩（上半部）与白云岩（下半部）呈明显的剥蚀面接触（红箭头），火山碎屑岩显示正粒序[58]；（h）喷爆岩，可见大量斑状方解石，红色箭头指示碎斑状颗粒数量逐渐减少至消失，准噶尔盆地吉木萨尔凹陷芦草沟组，J32 井，3 733.20 m，岩心手标本照片[63]；（i）对应 h 岩心手标本岩石薄片照片，准噶尔盆地吉木萨尔凹陷芦草沟组，J32 井，3 733.20 m，单偏光[63]；（j）对应图 i 中 j 框位置，发育碎斑状方解石，裂隙发育，准噶尔盆地吉木萨尔凹陷芦草沟组，J32 井，3 733.20 m，单偏光[63]

Fig. 1　Characteristic diagram of volcanic-hydrothermal sediments

(a)horizontally bedded shale with two periods of tuffaceous layers, the lower layer is a feldspar crystal tuff layer, and the upper layer is a glassy tuff layer, Chang 7 member, Ordos Basin, YY1 well, 228.44 m, planed-polarized light (PPL)[47]; (b)horizontally bedded shale with two periods of normal-graded volcanic crystal fragments, Chang 7 member, Ordos Basin, YY1 well, 229.60 m, PPL[47]; (c)normal-graded volcanic crystal fragments, Chang 7 member, Ordos Basin, YY1 well, 236.50 m, PPL[47]; (d)tuff of the lower crystal fragments in Figure a , Chang 7 member, Ordos Basin, YY1 well, 228.44 m, PPL[47]; (e)interbedded laminated volcaniclastic rock (white) and dolomite (dark brown), Lucaogou Formation, Santanghu Basin, M11 well, 2 944.80 m, PPL[58]; (f)enlargement of the f frame in e, showing angular feldspar grains (white), some with a chicken-bone structure (red arrow)[58]; (g)enlargement of the g frame in e, showing a clear erosional contact between the volcaniclastic rock (upper half) and the dolomite (lower half), with the volcaniclastic rock displaying normal grading[58]; (h)explosion breccia, with a large number of patchy calcite, red arrows indicating the gradual decrease to disappearance of patchy particles, Jimusaer Depression, Jung gar Basin, Lucaogou Formation, J32 well, 3 733.20 m, core photo[63]; (i)corresponding rock thin section photo of the hand specimen in h, Jimusaer Depression, Jung gar Basin, Lucaogou Formation, J32 well, 3733.2 m, PPL[63]; (j)corresponding to the j frame in Figure i, showing developed patchy calcite with developed fractures, Jimusaer Depression, Junggar Basin, Lucaogou Formation, J32 well, 3 733.20 m, PPL[63]

整体而言，火山—热液源细粒沉积物质包含复杂的矿物组成，矿物剥蚀、搬运痕迹较弱，整体分选差、磨圆度低，具有轻微的定向排列的特征，常呈正粒序纹层状、条带状分布于细粒沉积岩中。但不同的是，火山碎屑物质的发育规模往往大于喷流式沉积物和喷爆式沉积物，且物质组成更加多样，而喷流式沉积物和喷爆式沉积物常呈纹层状分布且物质组成单一。另外，喷爆式沉积物与火山碎屑物质、喷流式沉积物的矿物形态相比，更具备“碎斑状”的“爆破”特征。

2　细粒沉积岩典型物质的来源及其成因

2.1　黏土矿物来源及其成因

高岭石、蒙脱石、伊利石、绿泥石等是细粒沉积岩中常见的黏土矿物类型，不同的黏土矿物组合反映不同物质来源[19]。细粒沉积岩中的部分黏土矿物为陆源成因，其类型、数量受母岩性质、源区气候、风化强度等因素控制[18,64-66]。其中古气候条件是制约母岩风化方向、风化强度和黏土矿物类型的关键要素，不同的温度和湿度的二元组合能够导致母岩风化强度、

风化方向和黏土矿物类型发生改变。在不考虑气候条件、构造活动等因素的情况下，母岩性质则是影响黏土矿物生成的主要因素，通常沉积岩的抗化学风化能力强于火成岩类[67]，而火成岩中的原生矿物按照鲍温反应系列（图 2）[68]，从橄榄石到石英，其抗风化能力又逐渐增强[69]。

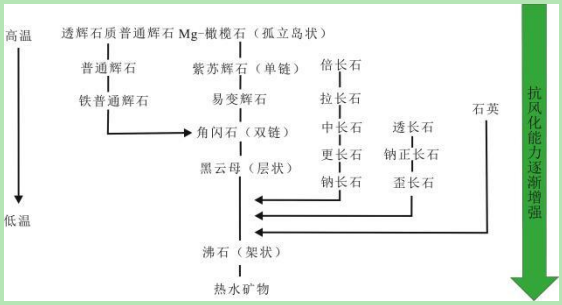

图 2　鲍温反应系列图及抗风化能力[68]

Fig. 2　Bowen's Reaction Series diagram and weathering resistance [68]

高岭石主要由花岗岩、花岗闪长岩等酸性、中性岩浆岩在温暖潮湿的气候条件下形成[70-71]，蒙脱石主要由陆源的中性岩浆岩和基性岩浆岩在干湿交替的气候条件或强季节性强降水环境下经过风化作用形成[72-75]。Robert *et al*.[76]认为半干旱地区蒙脱石结晶程度较高，因此其能够作为区域降水量的指示特征，此外 Jiménez-Espinosa *et al*.[77]认为与赤铁矿伴生形成的蒙脱石能够指示半干旱的气候条件。伊利石是典型的陆源黏土矿物，主要由陆地上的各种母岩经过风化作用形成[70-78]，干冷条件下淋滤作用较弱，伊利石的保存条件较好[71]，当气候向湿热条件转变时，伊利石的保存条件变差，逐渐向高岭石转变。绿泥石主要是在干燥寒冷气候条件下由低级变质岩、岩浆岩以及先前的沉积岩在化学风化作用受到抑制的条件下风化形成[70-71,79-80]。

另外，细粒沉积岩在成岩时期发生矿物之间的相互转化也是黏土矿物的重要成因之一。成岩演化时期，在一定的温压条件下有机质脱羧形成大量有机酸并释放 CO_2 对环境中的长石、云母进行溶解形成高岭石[81]；此外，当成岩时期具有钾源流体的情况下，偏基性的斜长石溶蚀后可直接沉淀形成伊利石[82]。除了其他矿物转化形成黏土矿物，成岩演化时黏土矿物之间也会发生转化，其遵循的规律一般是高岭石→蒙脱石→伊/蒙混层→伊利石、高岭石→伊利石[83]，通常这一过程也与长石的溶解共同发生，长石不断溶解为环境中供给 K^+，促进黏土矿物转化。随着研究的不断深入，黏土矿物演化及其组合已经成为表征细粒沉积岩成岩作用阶段及成熟度的指标，已有学者对黏土矿物类型和组合特征以及成熟度之间的关系进行了匹配与划分（图 3）[84]。

也有学者认为黏土矿物的来源与海底火山物质海解有关，大量学者研究发现在火山活动

强烈的海底，如太平洋中部、马里亚纳海槽等地区的蒙脱石含量较高，其主要由海底火山活动形成的基性火山物质在海底风化形成[85-87]。靳宁等[88]在研究帕里西维拉海盆北部表层沉积物的黏土矿物物质来源时，发现蒙脱石丰富的区域往往与火山玻璃丰富的区域相匹配，认为蒙脱石的物源与成因和火山活动有着密切关系，且研究区弱碱性、弱氧化性的沉积环境更适合火山物质蒙脱石化作用的发生和蒙脱石的保存。

图 3　黏土矿物与细粒沉积岩成岩演化等指标关系[84]

Fig. 3　The relationship between clay minerals and the diagenesis indicators of fine-grained sedimentary rocks[84]

随着研究的不断深入，前人对现代土壤、湖泊以及海洋的细粒沉积物进行研究发现，常见的蒙脱石、海泡石、坡缕石、伊利石等黏土矿物均能够由胞外聚合物（Extracellular Polymeric Substances，EPS）通过生物介导作用形成[89-92]。王杰等[93]在研究微生物对沙土强度的影响时，发现胶质芽孢杆菌生长活动形成的有机酸和 EPS 对环境中的硅酸盐矿物能产生一定的生物风化作用，部分硅酸盐矿物在风化溶蚀、络合作用下逐渐分解，形成充填在颗粒与颗粒之间的黏土矿物。

目前缺乏直接利用镜下形态特征分辨黏土矿物具体物源的研究方法，主要因为黏土矿物类型多样，产状和微结构特征复杂，单纯利用镜下识别不仅难度大、误差大，且缺乏定量数据反馈的能力。因此大多数黏土矿物溯源方法仍是通过乙二醇饱和处理、加热处理、XRD 特征谱线分析、Biscaye 方法等得到研究区黏土矿物的类型和相对含量，结合区域地质背景与研究区周边可能的黏土矿物物源区做对比，综合分析识别黏土矿物的物质来源[94-97]。另外，由于黏土矿物性质极不稳定，易受到氧化还原条件、水动力条件、水体 pH 值等环境条件影响以及有机质吸附作用、成岩作用、热液作用、地下水活动等后期改造作用影响，从而改变黏土矿物性质和其指示物质来源的信号[98-99]，因此目前涉及黏土矿物的物质来源研究往往围绕表层细粒沉积物和现代细粒沉积物展开[73,100-103]。

2.2　石英来源及其成因

石英作为细粒沉积岩重要的矿物组成，在细粒沉积学理论研究以及非常规油气资源勘探

开发中具有重要的研究意义。早期的研究常认为细粒沉积岩中的石英主要来源于陆源碎屑[104-105]，然而随着研究的不断深入，这一观点逐渐被推翻，Chen *et al.*[106]认为洋盆中的石英多来源于火山—热液活动；Schieber *et al.*[107]认为页岩中的石英除了陆源提供，浮游生物的蛋白石骨架溶解也能提供石英；Zhao *et al.*[108]认为石英不仅来源于浮游生物，还能来源于黏土矿物转化；Metwally *et al.*[109]认为石英来源于黏土矿物转化和长英质矿物的溶解以及交代作用；另外，Milliken *et al.*[110]研究发现美国晚白垩世的 Eagle Ford 页岩区域，自生石英的比例高达 85%，Ye *et al.*[111]研究认为我国四川盆地五峰组—龙马溪组页岩中自生石英的含量可达到 50%。综合上述观点，可将石英类型总结为：陆源碎屑石英、生物石英、火山—热液源石英、黏土矿物转化石英、长英质矿物溶蚀石英、交代石英等。

细粒沉积岩中的陆源碎屑石英具有较强的抗风化能力，在整体搬运过程中保存良好，常呈次圆状—次棱角状，粒级分布介于 10~50μm（图 4a）[20-21,112]。电子显微镜下，陆源碎屑石英颗粒无色透明，正交光下干涉色较淡，如：一级灰白、一级黄白、一级淡黄等，另外由于搬运作用、成岩作用的影响，陆源碎屑石英表面常有裂纹和溶蚀现象，部分石英边缘可见次生加大边（图 4b）[113-114]。通常，利用石英颗粒表面微形态特征能够分析其搬运方式[115]：风力搬运的陆源碎屑石英表面常见碟形撞击坑（图 4c）、新月形撞击坑（图 4d）、麻点等特征（图 4e）；水力搬运的陆源碎屑石英表面常见水下磨光面（图 4f）、直线或弯曲的撞击沟（图 4g）、V 形撞击坑（图 4h）等水力搬运特征[22-23,116-118]。

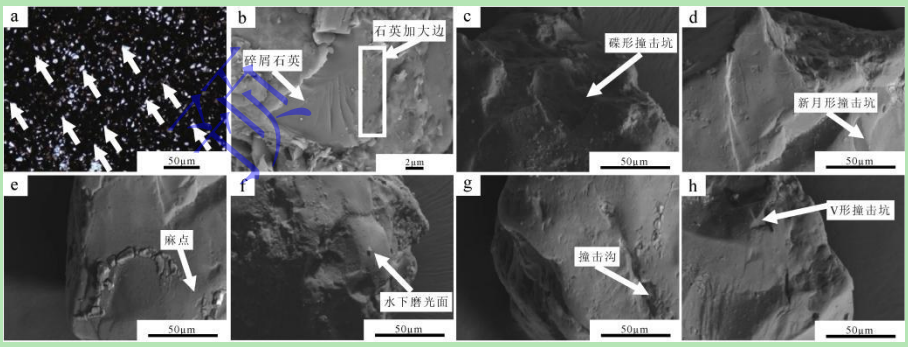

图 4　陆源碎屑石英特征图

（a）陆源碎屑石英（白色箭头所指），分选较好，呈次棱角状—次圆状均匀分布在细粒沉积岩中，黔北正安地区，龙马溪组，安页 2 井，单偏光[112]；（b）陆源碎屑石英伴生的石英加大边（白框内），沁水盆地山西组—太原组，扫描电镜[114]；（c）风力搬运陆源碎屑石英表面微型态—碟形撞击坑，扫描电镜[116]；（d）风力搬运陆源碎屑石英表面微型态—新月形撞击坑，扫描电镜[116]；（e）风力搬运陆源碎屑石英表面微型态—麻点坑，扫描电镜[116]；（f）水力搬运陆源碎屑石英表面微型态—水下磨光面，扫描电镜[116]；（g）水力搬运陆源碎屑石英表面微型态—撞击沟，扫描电镜[116]；（h）水力搬运陆源碎屑石英表面微型态—V 形撞击坑，扫描电镜[116]

Fig. 4　Characteristics of detrital quartz from terrestrial sources

(a)terrestrial detrital quartz (indicated by white arrows), well sorted, with subangular to subrounded shapes evenly distributed in fine-grained sedimentary rocks, in the Zheng'an area of Northern Guizhou, Longmaxi Formation, Anye-2 well, PPL[112]; (b)terrestrial

detrital quartz accompanied by quartz overgrowth (within the white frame), in the Qinshui Basin, Shanxi Formation - Taiyuan Formation, Scanning Electron Microscope (SEM)[114]; (c)aeolian transported terrestrial detrital quartz with surface micro-morphology - disc-shaped impact craters, SEM[116]; (d)aeolian transported terrestrial detrital quartz with surface micro-morphology - crescent-shaped impact craters, SEM[116]; (e)aeolian transported terrestrial detrital quartz with surface micro-morphology - pitted craters, SEM[116]; (f)hydraulic transported terrestrial detrital quartz with surface micro-morphology - subaqueous polished surfaces, SEM[116]; (g)hydraulic transported terrestrial detrital quartz with surface micro-morphology - impact grooves, SEM[116]; (h)hydraulic transported terrestrial detrital quartz with surface micro-morphology - V-shaped impact craters, SEM[116]

形成陆源碎屑石英的母岩在地质历史时期所经历的温度条件不同，阴极发光特征也不同，因此利用阴极发光特征能够分析陆源碎屑石英的母岩类型[111]。母岩为火成岩（经历温度>573 ℃）的石英阴极发光以蓝紫色为主[119-120]（图 5a）；母岩为变质岩（经历温度 300℃~573）的石英阴极发光以棕色、褐紫色为主（图 5b）[121-123]；母岩为沉积岩（经历温度<300 ℃）的石英阴极发光表现为不发光（图 5c）[121]。此外，利用 SEM-CL 图像和单色阴极发光光谱特征也能分析石英是否属于陆源碎屑：通常陆源碎屑石英表现为 SEM-CL 图像上的强发光和单色阴极发光光谱的双峰值，主峰为 625~650 nm，次峰出现为 420~450 nm 处[124-127]。

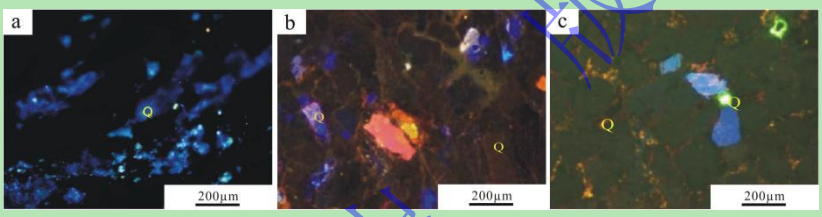

图 5　陆源碎屑石英阴极发光特征图

（a）陆源碎屑石英阴极发光呈蓝色，其母岩为岩浆岩，澜沧群沉积岩[119]；（b）陆源碎屑石英阴极发光呈棕褐色，偶见蓝紫色，母岩为变质岩和少量岩浆岩，苏峪口剖面[121]；（c）校育川剖面，陆源碎屑石英阴极发光呈棕褐色和不发光，偶见蓝紫色，证明母岩为变质岩、沉积岩和少量岩浆岩[121]

Fig. 5　Cathodoluminescence characteristics of detrital quartz from terrestrial sources.

(a)cathodoluminescence of terrestrial detrital quartz appears blue, its parent rock is igneous, Lancang Group sedimentary rocks[119]; (b)cathodoluminescence of terrestrial detrital quartz appears brown, occasionally blue-purple, parent rock is metamorphic rock and a small amount of igneous rock, Suyu Kou section[121]; (c)at the Xiaoyu Chuan section, the cathodoluminescence of terrestrial detrital quartz appears brown and non-luminous, occasionally blue-purple, indicating that the parent rocks are metamorphic rocks, sedimentary rocks, and a small amount of igneous rocks[121]

生物石英主要源于盆内的硅质生物躯壳，如：放射虫、海绵骨针、硅藻等硅质生物，属于内源沉积物质。硅质生物生长活动时从水体中汲取 Si^{4+}，将其在体内转化为性质不稳定的蛋白石-A，生物死亡后其沉积在水体底部，在早成岩阶段受到温度、压力等作用下，不稳定的蛋白石-A 逐渐向稳定的蛋白石-CT 转化，最终转化形成稳定的隐晶质、微晶以及粗晶石英[21,128-129]。生物石英一般具有两种常见的形式：一种是继承了生物原始结构、形态的石英（图 6a，b）[114,124,129-132]，另一种是受到水—岩作用溶解后经过重结晶作用形成的无生物结构的隐晶/微晶质石英集合体，常与沥青质体伴生（图 6c）[132]。通常生物石英在阴极射线照射下弱发光或不发光（图 6d）[114]，单色阴极发光光谱主峰在 580~620 nm 之间，次峰在

390~430 nm 之间[133]。

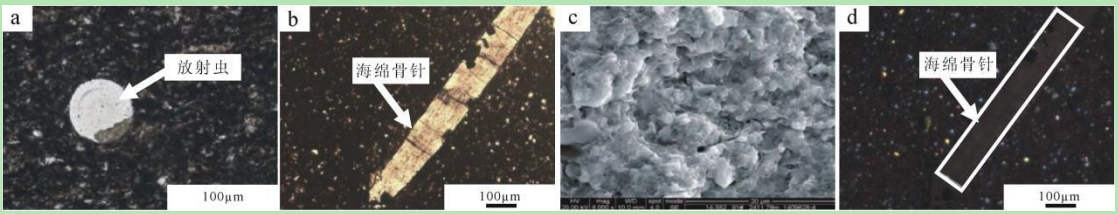

图 6　生物石英特征图

（a）放射虫石英，下扬子地区，高家边组，鼓地 1 井，1 222.00 m，单偏光[114]；（b）海绵骨针石英，重庆盆地东北部下志流统龙马溪组，单偏光[131]；（c）微晶石英集合体，表面光滑细腻，多为隐晶质，四川盆地五峰组—龙马溪组，扫描电镜[132]；（d）图（b）的阴极发光照片，白框对应（b）中的海绵骨针，阴极射线照射下表现为不发光[114]

Fig. 6　Cathodoluminescence characteristics of detrital quartz from terrestrial sources

(a)radiolarian quartz, in the Lower Yangtze region, Gaojiabian Formation, Gudi-1 well, 1222m, PPL[114]; (b)spicule quartz, in the northeastern Chongqing Basin, Lower Zhiliu System Longmaxi Formation, PPL[131]; (c)microcrystalline quartz aggregates, smooth and delicate surfaces, mostly cryptocrystalline, Sichuan Basin Wufeng Formation - Longmaxi Formation, SEM[132]; (d)cathodoluminescence photograph of Figure (b), the white frame corresponds to the spicules in (b), non-luminous under cathode ray irradiation[114]

火山—热液活动也是细粒沉积岩石英的重要来源，火山喷发带来的凝灰质物质是细粒沉积岩的重要物质组成，常呈条带状、纹层状分布（图 7a）[134]，其包含丰富的、性质极不稳定的火山玻璃[135-137]，在早成岩作用浅埋藏阶段，火山玻璃经历脱玻化转变为微晶石英[138]、长石等矿物以及非晶形态的二氧化硅。扫描电镜下可见火山—热液源石英呈微型条带状聚集（图 7b），也可见石英形成于孔、洞之中（图 7c）[139]。火山—热液源石英主要以两种形式存在，一种呈非晶形态，不规则球粒状、无棱角发育（图 7d，e）[137,139]；另一种常与长石、白云石、残留的火山物质共生的石英，其晶型较好，多呈短柱状而并非经典的六方柱状分布（图 7c，f）。当利用石英的晶体形态难以判断其为火山—热液源石英时，可以利用石英附近的非晶态物质能谱分析判断，一般硅铝比显示为与上地幔中的硅铝比相一致的 7~9，或远高于大陆地壳中 3.8 的硅铝比时，则证明石英为火山—热液来源[139]。

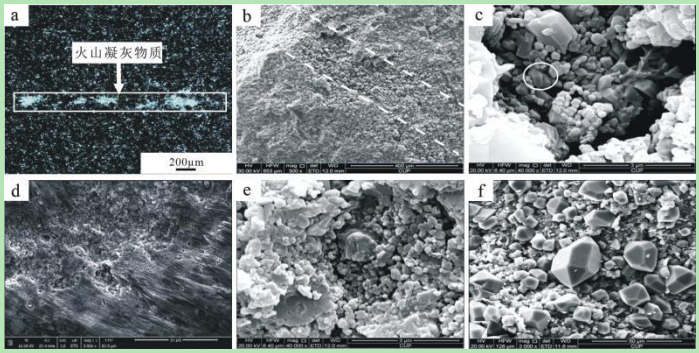

图 7　火山—热液作用石英特征图

（a）火山凝灰物质，呈纹层状分布，鄂西咸丰地区，五峰组—龙马溪组，鄂咸页 1 井，1 512.80 m，正交偏光[134]；（b）凝灰质细粒沉积岩，图中白色条带中间为石英聚集形成的条带，马朗坳陷芦草沟组，LU1 井，3 062.18 m，扫描电镜[139]；（c）凝灰岩，白圈为凝灰岩脱玻化形成自生石英，与长石共生形成于孔、洞之中马朗坳陷芦草沟组，LU1 井，3 060.63 m，扫描电镜[139]；（d）含云凝灰质物质脱玻化形成非晶体形态的二氧化硅，玛湖坳陷粉尘风城组，MY1 井，4 952.18 m，P_1f^1，扫描电镜[137]；（e）凝

灰物质脱玻化作用形成非晶态，不规则球粒状二氧化硅，马朗坳陷芦草沟组，LU1 井，3 060.63 m，扫描电镜[139]；（f）凝灰物质脱玻化形成晶型较好的，短柱状石英，与白云石、长石、残余火山物质共生，马朗坳陷芦草沟组，LU1 井，3 062.18 m，扫描电镜[139]

Fig. 7　Characteristics of hydrothermal-volcanic quartz

(a)volcanic ash material, distributed in a laminated pattern, in the western Hubei Xianfeng area, Wufeng Formation - Longmaxi Formation, EXY 1 well, 1 512.80 m, cross-polarized light (XPL)[134]; (b) tuffaceous fine-grained sedimentary rock, the white band in the middle of the picture is a band formed by the aggregation of quartz, Malang depression Lucaogou Formation, LU1 well, 3 062.18 m, SEM[139]; (c) tuff, the white circle is the self-formed quartz formed by the devitrification of tuff, coexisting with feldspar in pores and caves in the Malang depression Lucaogou Formation, LU1 well, 3 060.63 m, SEM [139]; (d) devitrification of tuff material containing cloud ash to form non-crystalline forms of silicon dioxide, Mahu depression dust wind city group, MY1 well, 4 952.18 m, P_1f^1, SEM[137]; (e) devitrification of tuff material to form amorphous, irregular spherical silicon dioxide, Malang depression Lucaogou Formation, LU1 well, 3 060.63 m, SEM [139]; (f) self-formed quartz formed by the devitrification of tuff material, with better crystallinity, short columnar quartz, coexisting with dolomite, feldspar, and residual volcanic material, Malang depression Lucaogou Formation, LU1 well, 3 062.18 m, SEM[139]

除了上述陆源、内源、火山—热液源所直接或间接向细粒沉积岩提供的石英外，成岩作用也是石英形成的重要方式之一，但其物源溯源难度大，因此难以划分至本文的三大物源方案之中。成岩过程中随着温度、压力的不断增大，黏土矿物逐渐从蒙脱石、伊/蒙混层、高岭石向伊利石转化[140]。该过程中黏土矿物不断从环境中汲取 K^+，并向环境中释放 Si^{4+}[141]，由于细粒沉积岩的渗透率极低，其释放的游离 Si^{4+}无法流动和扩散，因此逐渐沉积在原地，随着成岩作用的进行，一部分 Si^{4+}逐渐转化为自生石英充填于黏土矿物之间（图 8a，b）[16,35]。这一过程涉及大量钾的供应，通常钾来源于长石的溶解，当有机质进入生油窗时，有机质脱羧形成大量有机酸并释放 CO_2 对环境中的长石进行溶解，该过程不仅能直接向环境内输送硅质还能提供大量 K^+，促进黏土矿物转化释放大量硅质[142-143]。四川盆地自流井组常见大量生物介壳边缘发育石英，其是由介壳边缘的长石溶解、黏土矿物转化释放的硅质对介壳边缘的方解石交代所形成的成岩自生石英（图 8c）[144]。另外，在碱性的成岩条件下，陆源碎屑石英颗粒表面常被溶蚀产生孔隙，边缘溶蚀呈港湾状，当溶蚀的 Si^{4+}浓度达到饱和时，可形成石英次生加大边（图 8b）或以自生石英晶体独立存在[145]。

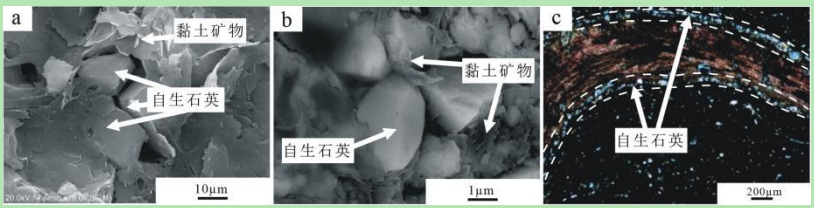

图 8　成岩作用石英特征图

（a）成岩自生石英，充填于黏土矿物之间，济阳坳陷沙四上亚段，NY1 井，3 456.50 m，扫描电镜[16]；（b）成岩自生石英，充填于黏土矿物之间，鄂尔多斯盆地延长组，G293 井，2 565.00 m，扫描电镜[35]；（c）硅质交代钙质形成的自生石英，石英在介壳边缘向内部生长（箭头所指虚线内），川北元坝地区侏罗统大安寨段，YL4 井，3 758.20 m，正交偏光[144]

Fig. 8　Diagenetic quartz characteristics diagram

(a)diagenetic self-formed quartz, filling between clay minerals, Jiyang depression Sha four upper sub-segment, NY1 well, 3 456.50 m,

SEM[16]; (b)diagenetic self-formed quartz, filling between clay minerals, Ordos Basin Yanchang Formation, G293 well, 2 565.00m, SEM[35]; (c)self-formed quartz formed by silicification of calcareous material, quartz growing from the edge of the shell to the inside (indicated by the dashed line in the arrow), in the Yuanba area of Northern Sichuan, Jurassic Da'anzhai segment, YL4 well, 3 758.20m, XPL[144]

2.3 长石来源及其成因

长石族矿物是细粒沉积岩储层中的重要骨架颗粒，大量的钻井岩心资料表明长石矿物广泛存在于古生代—新生代的相关细粒沉积地层中，例如：我国鄂尔多斯盆地上三叠系延长组[146]、渤海湾盆地沧东凹陷古近系孔二段[147]、四川盆地中侏罗世千佛崖组[148]、松辽盆地白垩系青山口组[149]、三塘湖盆地二叠系芦草沟组[150]等。作为细粒沉积岩重要的物质组成，长石在构造背景和物源区性质判识、沉积环境分析、古环境重建等方面有着不可忽视的研究意义。

通常，细粒沉积岩中的长石大部分来源于陆源物质风化，即陆源区母岩，特别是花岗岩和片麻岩，经过长期风化作用形成，伴随多种搬运介质搬运并进一步风化，最终形成细粒沉积岩的组成部分。相较于石英而言，长石族矿物的抗风化能力较弱，因此其在细粒沉积岩中的含量往往小于石英，而钾长石与钠长石相比具备更强的风化能力，这就导致细粒沉积岩中的斜长石含量随着陆源区距离的增加而逐渐减小，而钾长石的相对含量逐渐增加，通过这一特征并结合具体研究的实际地质条件、地质背景，能够对细粒沉积岩陆源区进行初步的判识[151]。但 Schieber *et al*.[107,152]在 1996 年和 2000 年研究北美泥盆系富有机质细粒沉积岩时，将与长石同属于硅酸盐矿物的石英作为研究对象，发现其含量不具备上述的传统沉积学理论所支撑的由陆源区向沉积中心递减的现象，并且石英颗粒多具备自生结构特征，而几乎无搬运特征，应是其他作用形成。因此，同上一小节石英的来源与成因一样，除了聚焦于传统陆源碎屑提供外，还应考虑其他来源。

随着研究的不断深入，众多学者一致认为火山—热液活动也是细粒沉积岩中长石矿物的重要物质来源之一。一方面，火山活动形成的火山碎屑物质和水下热液活动能够直接为细粒沉积岩“源—汇”系统提供长石矿物，如：我国准噶尔盆地、三塘湖盆地等盆地均发现以钠长石、方沸石为主的“白烟囱”型喷流式沉积物[56,59]；另一方面火山—热液活动也能够为细粒沉积岩中长石的形成提供物质基础[52]，经成岩作用阶段形成长石，如：玛湖凹陷风城组常见由火山活动带来的火山玻璃、玻屑、火山尘等在沉积埋藏后，经碱性流体作用下重结晶形成的长石[137]。

除此之外，近年来微生物形成长石的相关研究也越来越受到重视。碱性铁还原菌等微生物在其铁还原酶的作用下[153]，破坏蒙脱石结构 Fe（Ⅲ）进而导致蒙脱石中大量的 Al、Si

等元素释放到环境中，而微生物表面的大分子有机物（即 EPS）携带大量负电荷的官能团，能够有效吸附环境中的 Al^{3+}、Si^{4+}等元素，形成纳米级无定形 Al-Si 复合体，再经历脱水、熟化的等作用最终形成长石（图 9）[154]。

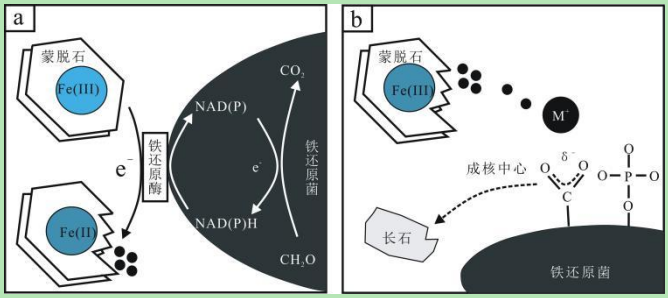

图 9　微生物介导长石形成机制[154]

（a）微生物体内有机质氧化产生电子经过铁还原酶传递给胞外含铁蒙脱石，导致蒙脱石结构被破坏；（b）蒙脱石释放的元素经过胞外聚合物吸附最终形成长石

Fig. 9　Mechanism of feldspar formation mediated by microorganisms[154]

(a)organic matter within microorganisms is oxidized to produce electrons that are transferred to extracellular iron-bearing montmorillonite through iron-reducing enzymes, leading to the destruction of the montmorillonite structure; (b)elements released from montmorillonite are adsorbed by extracellular polymers and ultimately form feldspar

2.4　碳酸盐矿物来源及其成因

碳酸盐矿物在碳酸盐质细粒沉积岩和混积细粒沉积岩中具有较高的含量分布，如我国渤海湾盆地始新统、南襄盆地渐新统湖相地层发育灰质细粒沉积岩[135,155-157]，江汉盆地古近系、渤海湾盆地沧东凹陷始新统、准噶尔盆地、三塘湖盆地中二叠统发育云质细粒沉积岩[135,158-163]，其往往受陆源碎屑供应、盆内环境条件以及火山—热液活动等多种因素共同控制形成（图 10）。

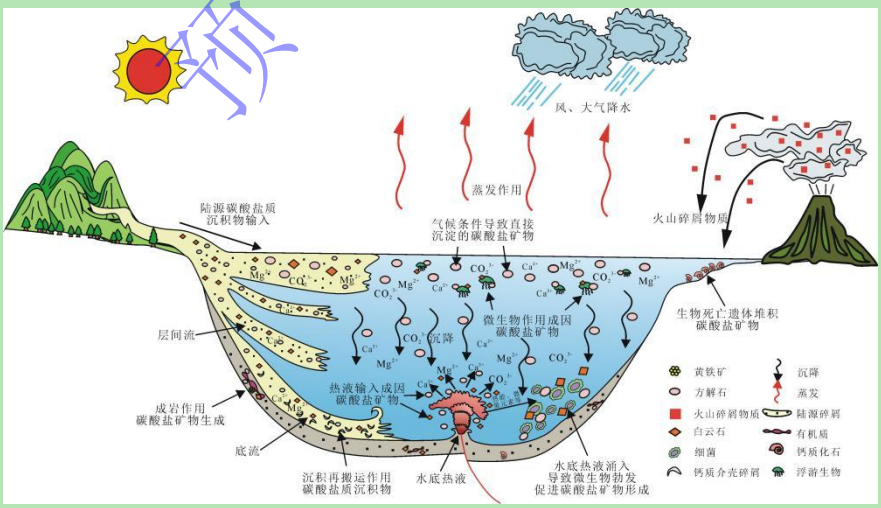

图 10　碳酸盐质细粒沉积物形成模式

Fig. 10　Formation patterns of carbonate fine-grained sediments

早期研究往往认为碳酸盐矿物主要由化学作用直接沉淀形成，但近年来学者们发现化学作用形成碳酸盐矿物的条件十分苛刻，当气候条件导致的蒸发作用非常强烈或者热液涌入水

体导致离子浓度局部过饱和时，才能通过化学作用形成大量碳酸盐质细粒沉积物，通常这类碳酸盐质细粒沉积岩有机质含量较低，如：江汉盆地潜江凹陷古近系发育大量低有机质韵律夹钙芒硝层状泥晶白云岩（图 11a）[164]，其形成原因可能与沉积时期亚热带干旱气候和封闭性高盐度湖水[165-166]导致的化学作用有关。另外，化学作用也常发生在成岩作用阶段：一方面，有机质成岩演化时，向环境内释放有机酸和 CO_2 对原有的碳酸岩矿物溶解，形成的流体经重结晶作用形成晶型较好的方解石[167]，常呈亮晶方解石纹层状分布（图 11b~d）[168-169]；另一方面，细粒沉积岩经过压实脱水，蒙脱石和伊利石等黏土矿物发生转化为环境卤水中释放大量 Mg^{2+}，形成富镁的高盐度白云石化流体，当白云石化流体与方解石进行深埋接触交代时，方解石逐渐转化为白云石，常呈中—粗晶、自形—半自形存在于细粒沉积岩中（图 11e，f）[170-172]。

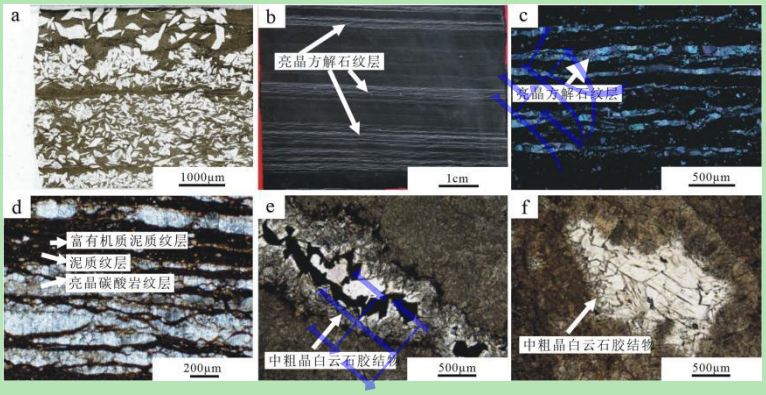

图 11　化学作用成因碳酸盐质细粒沉积物

（a）层状钙芒硝，芒硝结晶程度较好，江汉盆地潜江凹陷古近系，蚌页油 2 井，3 647.32 m，单偏光[164]；（b）纹层状灰质黏土岩，箭头所指为亮晶方解石纹层，川南地区五峰组—龙马溪组，W213 井，3 741.42 m，岩心照片[168]；（c）亮晶方解石纹层与黏土纹层互层，川南地区五峰组—龙马溪组，W213 井，3 741.42 m，正交偏光[168]；（d）亮晶方解石纹层与黏土纹层互层，渤海湾盆地东营凹陷沙三下亚段—沙四上亚段，正交偏光[169]；（e）埋藏成因形成的中—粗晶白云石胶结物，发育在孔隙边缘，具有明显的次生加大边，四川盆地震旦系灯影组，单偏光[172]；（f）埋藏成因形成白云石胶结物，四川盆地震旦系灯影组，单偏光[172]

Fig. 11　Chemically formed calcareous fine-grained sediments

(a)lamellar natrite, with well-formed crystals of natrite, in the Paleogene of the Qianjiang Depression of the Jianghan Basin, Bangye Oil 2 well, 3 647.32 m, PPL[164]; (b)laminated argillaceous limestone, with bright calcite laminae indicated by the arrow, in the Wufeng Formation - Longmaxi Formation of the Southern Sichuan area, W213 well, 3 741.42 m, core photo[168]; (c)alternating bright calcite laminae and argillaceous laminae, in the Wufeng Formation - Longmaxi Formation of the Southern Sichuan area, W213 well, 3 741.42 m, XPL[168]; (d)alternating bright calcite laminae and argillaceous laminae, in the lower submember of the Sha San and the upper submember of the Sha Si of the Dongying Depression, XPL[169]; (e)medium- to coarse-crystalline dolomite cement formed by burial genesis, developed at the edge of pores, with distinct secondary enlargement margins, from the Sinian Doushantuo Formation in the Sichuan Basin, PPL[172]; (f)dolomite cement formed by burial genesis, from the Sinian Doushantuo Formation in the Sichuan Basin, PPL[172]

近年来，众多学者围绕微生物在碳酸盐矿物形成中起到的作用，开展了大量研究工作，发现碳酸盐矿物的形成和盆内微生物化学作用密切相关[173-175]。一方面：水体中的浮游生物、

细菌，如浮游藻、蓝细菌等通过新陈代谢降低 CO_2 分压，导致水体 pH 值升高，HCO_3^-向 CO_3^{2-}方向转化，促进碳酸盐矿物形成（图 12a，b）[37,176-177]。通常，这类碳酸盐矿物具有明显的季节性差异，夏季水体生物勃发、蒸发作用强，易形成较厚的、颜色较浅的碳酸盐质细粒沉积纹层；而冬季水体生物大量死亡、蒸发作用弱，易形成较薄的、颜色较深的、由碳酸盐矿物、黏土矿物和生物死亡后形成的有机质共同组成的纹层（图 13a）[178-179]。另一方面，生物分泌的大分子有机物附着在生物表面形成的胞外聚合物（EPS）在碳酸盐矿物的形成中也扮演着重要角色[175,180-181]。EPS 含有带负电荷的官能团，能够结合水中的金属阳离子形成以生物细胞壁为基底的方解石、白云石等碳酸盐矿物（图 12c）[182-185]，当矿物形成后，成核基底有机质和 EPS 降解形成遗留的小孔（图 13b）。因此，微生物活动导致 EPS 微域的 pH 值局部增加，能够诱导形成无定形方解石与 EPS 大分子混合物产生纳米级方解石球体（图 13c，d），如渤海湾盆地东营凹陷沙河街组中的纳米级簇状、哑铃状方解石[175,186]；也能够诱导方解石围绕微生物沉淀，其核心为球状、哑铃状微生物（图 13e）[172,187]。除此之外，微生物硫酸盐还原作用和甲烷生成作用也能影响白云石的形成，通常，这种生物成因的白云石化作用主要用于解释非碱性微咸水—咸水湖相深水富有机质含泥白云岩或云质细粒沉积岩中的白云石成因，常与菱铁矿、黄铁矿伴生形成[188-189]。

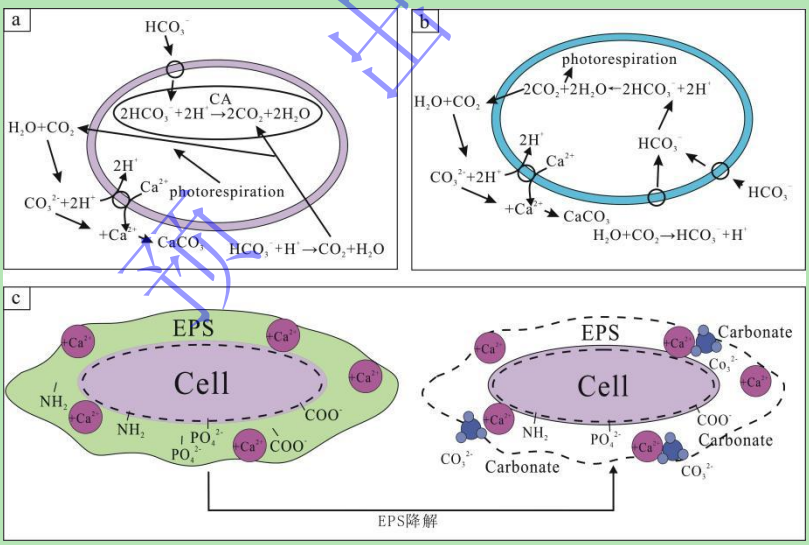

图 12　微生物化学作用形成碳酸盐矿物理论模型

（a）浮游藻生物化学作用形成方解石理论模型[37]；（b）蓝细菌生物化学作用形成方解石理论模型[37]；（c）微生物胞外聚合物促使碳酸盐矿物沉淀理论模型[185]

Fig. 12　Theoretical models for the formation of carbonate minerals by microbial chemical action

(a)theoretical model for the formation of calcite by planktonic algae through biochemical action[37]; (b)theoretical model for the formation of calcite by cyanobacteria through biochemical action[37]; (c)theoretical model for the precipitation of carbonate minerals induced by microbial extracellular polymers[185]

另外，盆内生物作用可直接为细粒沉积岩提供碳酸盐矿物：软体动物贝壳、轮藻、珊瑚

等生物死亡后遗体堆积直接可以形成方解石、文石、一水合碳酸钙等碳酸盐矿物[188]。这类碳酸盐矿物一定程度上保留着生物的原始形态（图 13f~h）[190-192]，广泛发育在巴西桑托斯盆地阿普特阶/巴雷姆阶 Itapema 组[193]、美国堪萨斯州下二叠统[194]以及我国四川盆地自流井组[195]、千佛崖组[196]、茅口组[197]、松辽盆地青山口组[198]、嫩江组[199]、羌塘盆地中侏罗统布曲组[200]、准噶尔盆地芦草沟组[201]、渤海湾盆地沙河街组[202]等细粒沉积地层中。

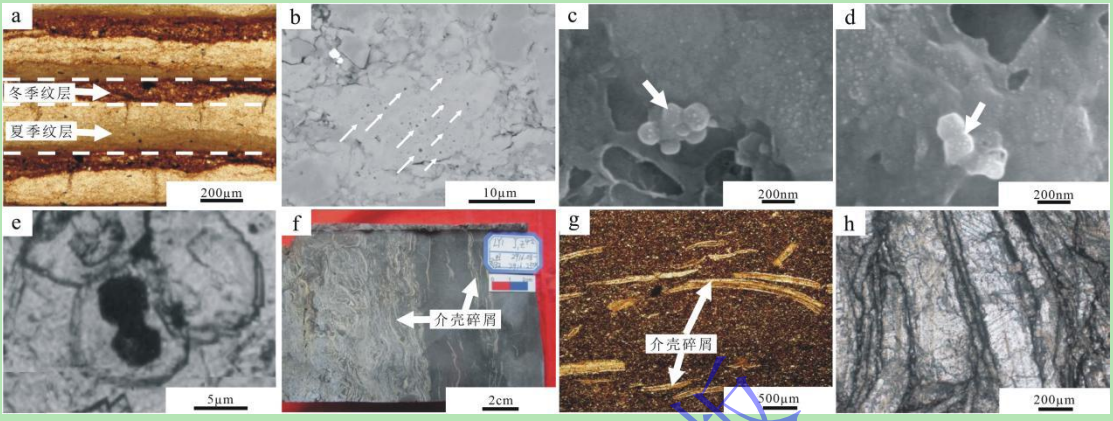

图 13　生物化学成因及生物成因碳酸盐矿物

（a）季节韵律性碳酸盐质细粒沉积岩，夏季浅色微亮晶方解石纹层和冬季褐色泥晶方解石纹层相互互层，束鹿凹陷 Es_3^L，ST1H 井，4 206.60 m，单偏光[178]；（b）EPS 介导作用形成的微亮晶方解石，白色箭头所指为有机质降解遗留的小孔，束鹿凹陷 Es_3^L，ST1H 井，4 206.20 m，氩离子抛光扫描电镜[32]；（c）簇状方解石，由多个纳米级球状方解石组成（白色箭头），东营凹陷沙河街组，扫描电镜[186]；（d）哑铃状方解石，由两个纳米级球状方解石组成（白色箭头），东营凹陷沙河街组，扫描电镜[186]；（e）微生物化学作用形成的微生物白云石，其内部保留微生物的原始形态[187]；（f）介壳泥岩，介壳排列杂乱无序，川北阆中地区大安寨二亚段，2 916.12~2 916.25 m，岩心照片；（g）含介壳粉砂质黏土岩，见介壳碎片呈漂浮状分布在细粒沉积岩中，仪陇—营山地区侏罗系大安寨段，平安 1 井，3 173.60 m，单偏光[191]；（h）介壳形成的亮晶方解石组成的介壳灰岩，元坝地区大二亚段，Y2 井，3 903.99 m，单偏光[192]

Fig. 13　Biochemically and biologically formed carbonate minerals

(a)seasonal rhythmic carbonate fine-grained sedimentary rocks, with light-colored microcrystalline calcite laminae in summer and brownish micritic calcite laminae in winter, Shu Lu Depression Es_3^L, ST1H well, 4 206.60 m, PPL[178]; (b)microcrystalline calcite formed by EPS-mediated action, with small holes left by the degradation of organic matter indicated by the white arrow, Shu Lu Depression Es_3^L, ST1H well, 4 206.20 m,argon ion polishing scanning electron microscope (AIP - SEM)[32]; (c)clustered calcite, composed of multiple nanoscale spherical calcite (indicated by the white arrow), in the Shahejie Formation of the Dongying Depression, SEM[186]; (d) dumbbell-shaped calcite, composed of two nanoscale spherical calcite (indicated by the white arrow), in the Shahejie Formation of the Dongying Depression, SEM [186]; (e)microbially formed dolomite through microbial chemical action, with the internal preservation of the original microbial morphology[187]; (f)shelly mudstone, with shells arranged in a disorderly manner, in the second member of the Da'an Zhai of the Northern Sichuan Langzhong area, 2 916.12~2 916.25m, core photo; (g)shelly silty claystone, with shell fragments floating in fine-grained sedimentary rocks, in the Jurassic Da'an Zhai section of the Yilong-Yingshan area, Ping'an 1 well, 3 173.60 m, PPL[191]; (h)shelly limestone composed of bright calcite formed by shells, in the second member of the Yuanba area, Y2 well, 3 903.99m, PPL[192]

除了生物化学作用、生物作用外，盆内的沉积物质再搬运沉积作用也是方解石、白云石等碳酸盐质细粒沉积物的重要成因机制[29]，如：东营凹陷南坡陈官庄地区沙河街组四段上亚段的混积细粒沉积岩中可见大量碳酸盐质砾屑颗粒（图 14a）[203]，即原先形成的沉积物质经过风暴侵蚀、破碎后重新沉积形成碳酸盐质沉积物。

陆源物质的输入同样也会对碳酸盐矿物的形成产生影响[29]。陆源区灰岩、白云岩、大理岩、玄武岩、碳酸岩等在风化淋滤过程中释放大量 Ca^{2+}、Mg^{2+}能为盆内碳酸盐矿物的形成提供丰富的物质基础[8]。通常情况下，陆源区以丰富的碳酸盐矿物组成的岩石为主时，盆区内具备形成大量碳酸盐岩的条件；当陆源区既有碳酸盐矿物又有硅质碎屑基岩时，盆内形成的碳酸盐岩规模会受到源区风化强度、物质输入类型以及构造特征等因素控制；当陆源区的碳酸盐矿物组成的岩石含量极少时，盆内缺乏 Ca^{2+}、Mg^{2+}等离子的供给，往往很难形成规模性的碳酸盐矿物[29]。另外，富含碳酸盐矿物的陆源区受到强构造活动、较为干旱的气候条件等因素的影响，能够直接为较近的盆内输入大量分选、磨圆较差的陆源碳酸盐质碎屑[24-26]，在东营凹陷沙三下亚段，可见大量分选、磨圆较差的云质碎屑与长英质矿物、黏土矿物共同沉积（图 14b，c）[32]。

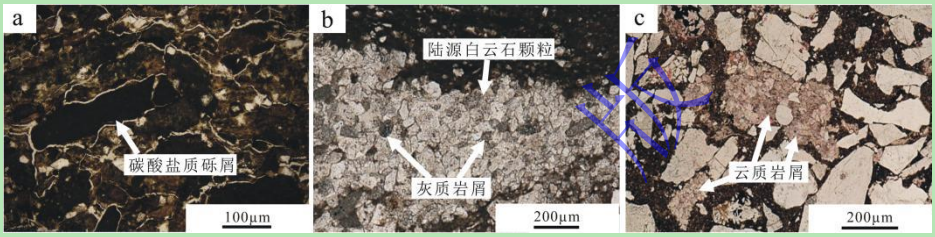

图 14　机械作用成因碳酸盐质沉积物特征图

（a）含粉砂砾屑泥晶灰岩，可见碳酸盐砾屑，东营凹陷南坡陈官庄地区沙河街组四段上亚段，G3 井，1 940.23~1 940.25 m，单偏光[203]；（b）陆源白云石颗粒夹灰质岩屑，束鹿凹陷 Es_3^L，ST3H 井，3 907.20 m，单偏光[32]；（c）白云石晶体组成的云质岩屑与周围磨圆度低的陆源长英质矿物共同沉积，东营凹陷 Eq_3^L，Y891 井，单偏光[32]

Fig. 14　Characteristics of mechanically formed carbonate sediments

(a)silty calcareous mudstone with gravel, visible carbonate gravel, in the upper submember of the fourth member of the Shahejie Formation of the southern slope of the Dongying Depression, Chen Guanzhuang area, G3 well, 1 940.23~1 940.25 m, PPL[203]; (b)terrestrial dolomite grains interbedded with argillaceous rock fragments, in the Shu Lu Depression Es_3^L, ST3H well, 3907.20m, PPL[32]; (c)dolomitic rock fragments composed of dolomite crystals and low-roundness terrestrial feldspathic minerals co-deposited, in the Dongying Depression Eq_3^L, Y891 well, PPL[32]

除了内源与陆源，火山—热液活动也是碳酸盐矿物的重要物质来源[59]。火山—热液活动可向盆内提供 Ca^{2+}、Mg^{2+}等离子并提高环境中 CO_2 含量以及水体的 pH 值，从而营造出更加适合碳酸盐矿物形成的环境[30,204-205]。一方面，水底热液的注入能够提高周围区域 Ca^{2+}、Mg^{2+}、Fe^{2+}、CO_3^{2-}等离子浓度和水体温度，促进富含 Fe、Mg 的方解石、白云石等碳酸盐矿物直接沉淀[59]，通常这类白云石晶体中的流体包裹体均一温度在 167℃~283℃，呈负偏态分布，55%的温度在 160℃~200℃，表明白云石在高温下形成，另外常伴生硅灰石、钠长石、重晶石、钠沸石、菱镁矿、地开石或立方黄铁矿等正常湖相沉积物中罕见的热液矿物[190]。另一方面，水底热液向四周流散，提高水底温度的同时也带来丰富的微量元素，促进微生物的勃发，进而促进碳酸盐矿物和有机质大量生成[206]。我国三塘湖盆地条湖—马朗坳陷芦草

沟组二段[150]、玛湖坳陷风城组[207]、准噶尔盆地吉木萨尔凹陷[30]等受火山—热液活动影响的细粒沉积岩中常见火山—热液活动影响下形成的白云石、方解石呈层状发育（图 15a，b），部分碳酸盐矿物与有机质共同发育（图 15c，d）。除此之外，火山—热液活动还能直接向盆内输入碳酸盐物质，在我国准噶尔盆地吉木萨尔凹陷细粒沉积岩中常见喷爆式方解石、白云石等碳酸盐矿物呈不规则碎斑状与细粒沉积物共同沉积（图 15e，f）[10,63,208]。

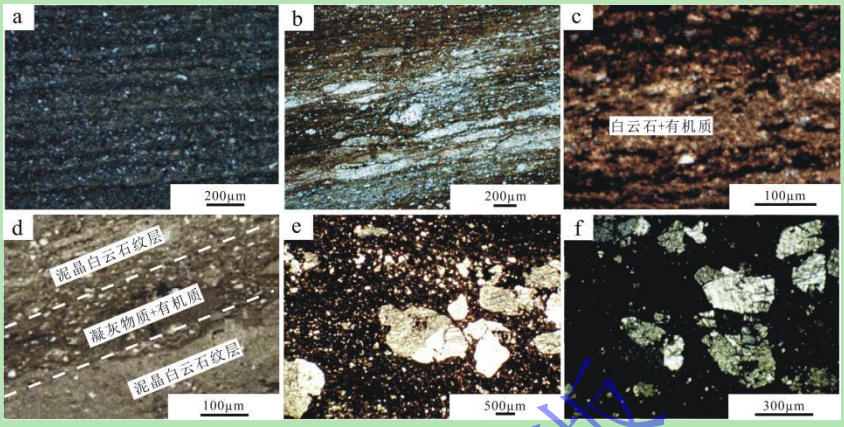

图 15　火山—热液作用碳酸盐质沉积物特征图

（a）纹层状白云质凝灰岩，显微层状构造，玛湖凹陷风城组，风南 1 井，4 338.19 m，正交偏光[207]；（b）含凝灰质藻云岩（浅褐色）夹凝灰质纹层（白色），准噶尔盆地吉木萨尔凹陷，吉 174 井，3 224.30 m，单偏光[30]；（c）纹层状白云质凝灰岩，白云石颗粒与长英质混杂，见有机质呈层状发育，马 78 井，3 048.00 m，单偏光[163]；（d）纹层状凝灰质白云岩，凝灰质与有机质层和泥晶白云石纹层互层，三塘湖盆地条湖—马朗凹陷芦草沟段，凝灰质白云岩，L1 井，3 079.13 m，单偏光[163]；（e）碎斑状喷爆式方解石，呈不规则颗粒以及集合体形态产出，准噶尔盆地吉木萨尔凹陷芦草沟组，上油层段，J174 井，3 197.00 m，单偏光[10]；（f）碎斑状喷爆式方解石，方解石呈不规则角砾状发育，可见粒内破裂现象，基质主要成分为白云石、铁白云石、方解石、钠长石、正长石和石英等，准噶尔盆地吉木萨尔凹陷，单偏光[208]

Fig. 15　Characteristics of carbonate sediments formed by volcanic-hydrothermal action

(a)laminated dolomitic tuff, with microlaminated structure, in the Fengcheng Formation of the Mahu Depression, Fengnan 1 well, 4 338.19 m, XPL[207]; (b)algal dolostone containing tuffaceous material (light brown) interbedded with tuffaceous laminae (white), in the Jimusaer Depression of the Junggar Basin, Ji 174 well, 3 224.30 m, PPL[30]; (c)laminated dolomitic tuff, with dolomite grains intermingled with feldspathic minerals, showing organic matter developed in layers, Ma 78 well, 3 048.00 m, PPL[163]; (d)laminated tuffaceous dolomite, with tuffaceous and organic layers and micritic dolomite laminae, in the Tiaohu-Malan Depression of the Santanhu Basin, tuffaceous dolomite, L1 well, 3 079.13 m, PPL[163]; (e)brecciated explosive calcite, irregular granular and aggregate forms, in the Licaogou Formation of the Jimusaer Depression of the Junggar Basin, upper oil layer, J174 well, 3 197.00 m, PPL[10]; (f)brecciated explosive calcite, calcite developed in an irregular angular breccia, with grain internal fractures, the matrix mainly composed of dolomite, ankerite, calcite, albite, orthoclase, and quartz, etc., in the Jimusaer Depression of the Junggar Basin, PPL[208]

2.5　黄铁矿来源及其成因

近年来黄铁矿在细粒沉积岩相关研究中得到广泛重视，其作为盆内金属硫化物的主要载体，在细粒沉积岩中广泛存在，具有指示沉积环境、成岩演化等作用[209-211]。通常细粒沉积岩中的黄铁矿以边缘较平直、晶体形态多样的自形黄铁矿（图 16a，b）[212]、大小均匀的微粒组成的草莓状黄铁矿（图 16c，d）[129,213]以及交代其他矿物所形成的交代型黄铁矿（图 16e，f）为主[214-216]。

铁元素和硫元素作为黄铁矿的重要成矿元素，是研究黄铁矿物质来源的关键。铁来源多样，包含河流输入、大气输入、冰川融解所带来的陆源铁元素、盆内沉积物质再循环的铁元素以及火山—热液活动输入的铁元素[217-219]，其在盆内以溶解铁、胶体铁、颗粒铁三种形式存在[220-221]。Fe^{3+}转化为 Fe^{2+}按照生物参与与否可将该过程划分为生物途径和非生物途径，其中生物途径主要以异化铁还原为主：地杆菌科（*Geobacteraceae*）、希瓦氏菌属（*Shewanella*）等特定细菌通过代谢活动利用细胞外的铁氧化物作为电子最终受体产生能量，将 Fe^{3+}还原成 Fe^{2+}[222]。而非生物途径主要是铁穿梭机制为主，在这个过程中 Fe^{3+}从沉积盆地的边缘较浅的水域被运输到盆地的更深处，穿越化学跃层还原成 Fe^{2+}[223-224]。

在研究黄铁矿物质来源时，相较于铁元素，学者们往往更加关注硫元素的来源和还原机制[225]。硫元素的来源与铁元素相似[219]，其还原作用主要依赖微生物硫酸盐还原作用（MSR）和硫酸盐热化学还原作用（TSR）[226-228]。其中 MSR 主要发生在浅埋藏带，按照反应的埋藏深度、参与硫酸盐还原反应物质、反应产物不同可以分为细菌硫酸盐还原作用（BSR）和甲烷厌氧氧化—硫酸盐还原作用（AOM-SR）。BSR 主要受到氧化还原界面、生物含量、硫酸盐浓度等方面控制[228-229]。开放环境中，氧化还原界面通常在水—沉积物界面以下；而在封闭环境中，氧化还原界面往往在水体中[230]。当细菌处于氧化还原界面以下、温度高于 0 ℃且不超过 80℃时，由细菌作为介导发生硫酸盐—碳氢化合物氧化还原反应形成黄铁矿中的硫元素（公式（1））[230]。由于 BSR 主要发生于沉积水体中以及浅埋藏带中，因此形成的草莓状黄铁矿粒度通常较小（平均小于 7.7 μm）（图 16c，d）[209,231]。

$$2CH_2O+SO_4^{2-}\rightarrow 2HCO_3^-+H_2S \quad (1)$$

AOM-SR 不受到氧化还原界面的控制，主要在更深部的硫酸盐—甲烷转换带（SMTZ）发生硫酸盐的还原作用（图 17）[219,232-234]。深部生成的甲烷沿着沉积物的孔隙向上运移扩散，与向下扩散的硫酸盐相遇，在还原细菌的作用下形成硫化氢[235]，因此该方式形成的黄铁矿通常受到沉积物孔隙通道的限制而呈管状或者棒状（图 16g）[224,236-237]。另外，随着埋深的改变经历 AOM-SR 作用形成的草莓状黄铁矿也会不断生长直至形成自型黄铁矿[232,238]。BSR 与 AOM-SR 发生的反应深度不同，经历过 BSR 作用所形成的黄铁矿在埋藏过程中经历 SMTZ 也会发生过度生长的现象（图 16h）[237]，因此 AOM-SR 形成的黄铁矿粒度偏大，平均大于 20 μm[239]。

TSR 并不涉及生物作用，是在达到一定温度（大于 140 ℃）才能够开始进行的硫酸盐还原作用，200 ℃左右是其反应作用效率最高的温度[240-245]。该反应的发生深度一般大于 MSR 的发生深度，是温度控制下的有机质还原硫酸盐作用（公式 2）[230,234-235]。TSR 反应形

成的黄铁矿在细粒沉积岩中主要以过度生长的自形黄铁矿、继承交代矿物形态的交代型黄铁矿（图 16e）以及过度生长的草莓状黄铁矿（图 16i）为主[209,246]。前人研究表明，除了深度和温度控制 TSR 反应的发生外，有机质的类型、环境 pH 值、硫酸盐类型也控制着该反应发生的强度[247-251]。

$$\sum CH+2CaSO_4 \rightarrow 2CaCO_3+2H_2S+CO_2 \quad （2）$$

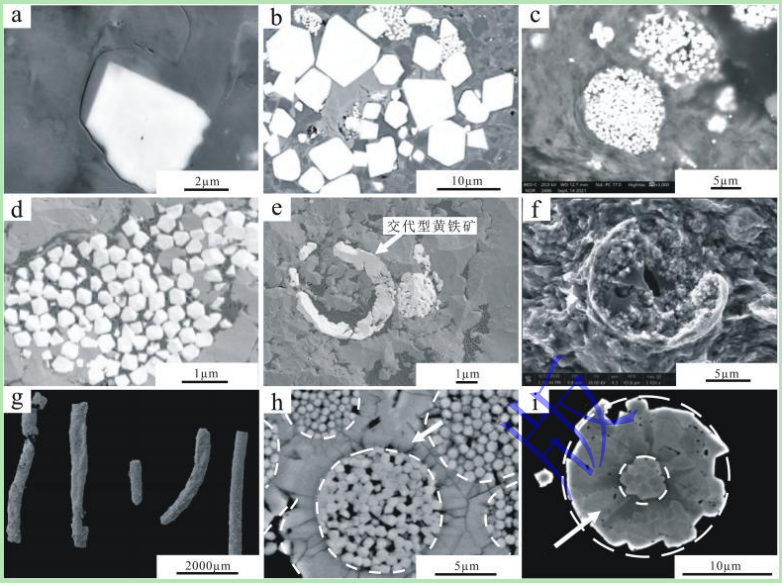

图 16　不同类型黄铁矿及其特征

（a）自型单晶黄铁矿，边缘平直，四川盆地泸州 I 区 Y101-01 井，五峰组龙一 $_1$ 亚段，3 744.51 m，扫描电镜[212]；（b）自型黄铁矿，边缘平直，四川盆地泸州 I 区 Y101-03 井，五峰组龙一 $_1$ 亚段，3 744.51 m，扫描电镜[212]；（c）草莓状黄铁矿，西湖凹陷平湖斜坡北段，KB1 井，P8 砂组，背闪射扫描电镜[213]；（d）草莓状黄铁矿，形成时期早于自生石英，粒径约 3 μm，川南地区，L202-84B，龙一 $_1$，4 322.26 m，扫描电镜[131]；（e）交代型黄铁矿，黄铁矿交代生物腔体，形成保留部分生物结构的黄铁矿，川南地区，L204-35JX，五峰组，3 845.64 m，扫描电镜[131]；（f）交代型黄铁矿，黄铁矿交代生物外壁与体腔，可见黏土矿物围绕藻类生物体腔生长，鄂尔多斯盆地，CY1 井，长 7_3 亚段，扫描电镜[214]；（g）AOM-SR 作用影响下的管状、棒状黄铁矿集合体，扫描电镜[236]；（h）经过 AOM-SR 作用影响的过度生长黄铁矿（箭头所指的白色虚线内），具再生长结构，扫描电镜[237]；（i）过度生长型草莓状黄铁矿，白色箭头所指的虚线区域内为经 TSR 作用后过度生长的黄铁矿，大唐坡组灰色页岩，埃迪卡拉纪，华南地区，扫描电镜[246]

Fig. 16　Different types of pyrite and their characteristics

(a)autogenetic single-crystal pyrite with straight edges, in the Yulin I area of the Sichuan Basin, Y101-01 well, Wufeng Formation - Long$_1$^{1} Submember, 3 744.51 m, SEM[212]; (b)autogenetic pyrite with straight edges, in the Yulin I area of the Sichuan Basin, Y101-03 well, Wufeng Formation - Long$_1$^{1} Submember, 3 744.51 m, SEM[212]; (c)strawberry-like pyrite, in the northern section of the Pinghu Slope in the Xihu Depression, KB1 well, P8 sand group, backscattered electron scanning microscope (BSEM)[213]; (d)strawberry-like pyrite, formed earlier than authigenic quartz, with a grain size of about 3μm, Southern Sichuan area, L202-84B, Long$_1$^{1}, 4 322.26 m, SEM [131]; (e)metasomatic pyrite, pyrite replacing biological cavities, forming pyrite that retains part of the biological structure, Southern Sichuan area, L204-35JX, Wufeng Formation, 3 845.64 m, SEM[131]; (f)metasomatic pyrite, replacing the outer wall and body cavity of organisms, with clay minerals growing around the body cavity of algae, Ordos Basin, CY1 well, Chang7$_3$ Submember, SEM [214]; (g)tubular and rod-shaped pyrite aggregates affected by AOM-SR, SEM[236]; (h)overgrown pyrite affected by AOM-SR (indicated by the white dashed line within the arrow), with a regrown structure, SEM[237]; (i)overgrown strawberry-like pyrite, the area within the dashed line indicated by the white arrow is the overgrown pyrite after TSR, in the grey shale of the Datangpo Formation, Ediacaran Period, South China, SEM[246]

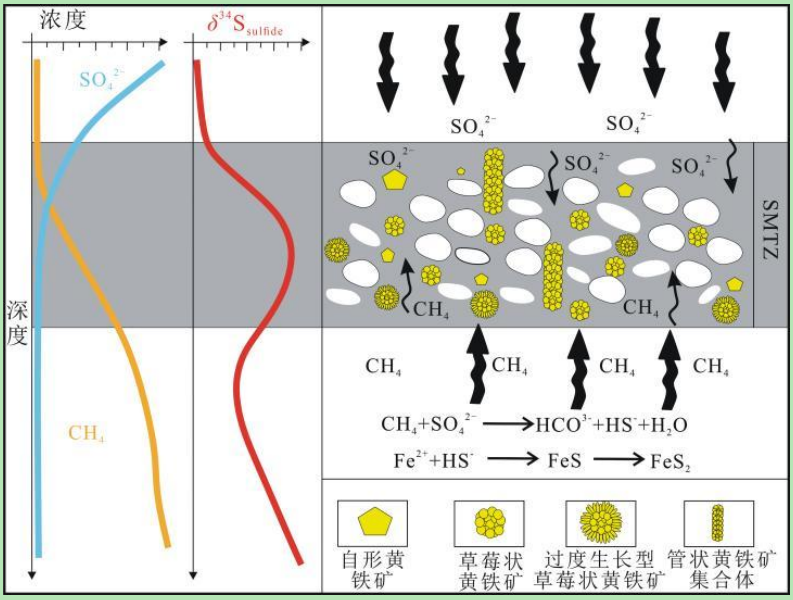

图 17　甲烷厌氧氧化-硫酸盐还原作用（AOM-SR）模式图[219]

Fig. 17　Schematic diagram of anaerobic oxidation of methane coupled to sulfate reduction (AOM-SR)[219]

2.6　有机质来源及其成因

细粒沉积岩中蕴含着丰富、多样的有机质，但目前并没有针对细粒沉积岩的有机质统一划分方案，大多数学者仍采取的是煤岩学中的有机质划分理论，将细粒沉积岩中的有机质划分为镜质体、惰质体、类脂体、动物有机碎屑以及次生有机质 5 大显微组分[27,252-253]，利用镜下观察有机质显微组分特征是最直接有效的物源研究方法，其各特征总结如下。

镜质体是随陆源碎屑一起搬运到盆内的陆源高等植物的茎、叶、木质纤维组织凝胶化形成的有机显微组分[27]，常在煤系细粒沉积地层中出现，物源可以追溯到靠近盆内水体的沼泽以及临近的陆源区域，按照形态可分为结构镜质体和无结构镜质体。结构镜质体具有较清晰的轮廓和更深的颜色，具长条状、网格状、块状等形态（图 18a，b）[254-255]。而无结构镜质体由于其粒度较小，常以颗粒状分散于细粒沉积岩基质中，很少具备明显的细胞结构（图 18c，d）[256-257]，镜下鉴别十分困难，因此难以对其显微组分进行准确划分[27]。

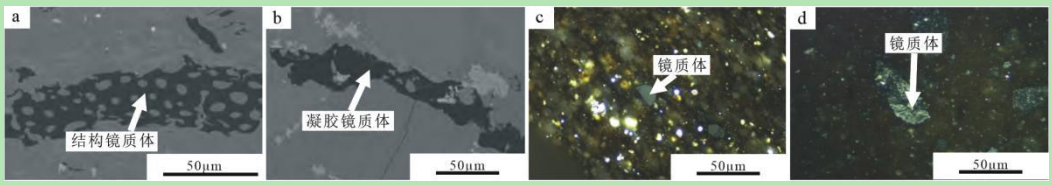

图 18　细粒沉积岩中镜质体特征

（a）网格状结构镜质体，细胞结构保留完好，武宁盆地武南区块，石炭—二叠系太原组—山西组[254]；（b）条带状凝胶镜质体，武宁盆地武南区块，石炭—二叠系太原组—山西组[254]；（c）无结构碎屑镜质体，美国 Illinois 盆地 New Albany 页岩，油浸反射光[256]；（d）无结构碎屑镜质体，川东—黔东南龙潭组，M1 井[257]

Fig. 18　Characteristics of vitrinite in fine-grained sedimentary rocks

(a)reticulated structure of vitrinite, with well-preserved cellular structure, in the Wuning Basin, Wuning South Block,

Carboniferous-Permian Taiyuan Formation-Shanxi Formation[254]; (b)banded gel vitrinite, in the Wuning Basin, Wuning South Block, Carboniferous-Permian Taiyuan Formation-Shanxi Formation[254]; (c)structureless detrital vitrinite, in the New Albany Shale of the Illinois Basin, USA, oil-immersion reflected light[256]; (d)structureless detrital vitrinite, in the Longtan Formation of the Eastern Sichuan-Southeast Guizhou area, M1 well[257]

惰质体来源与镜质体相似，均来自陆源高等植物，但不同的是惰质组在沉积前经历过丝炭化作用的氧化，因此其组分性质更加稳定，其最常见的显微组分是植物细胞形态保存较好的丝质体，纵断面呈纤维状，常顺层排列（图 19a~c）[258-259]，横断面常呈整齐的筛网结构，并被其他矿物充填（图 19d）[255]。除此之外，半丝质体、碎屑惰质体等也是细粒沉积岩中常见的惰质体类型。

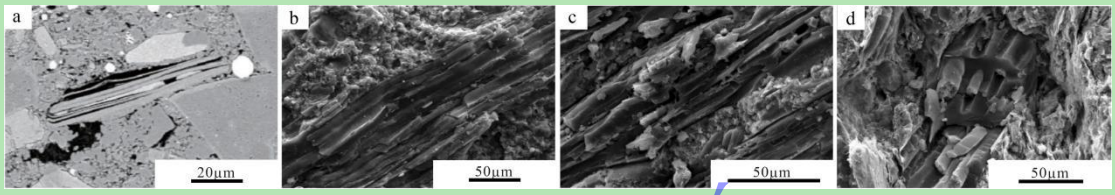

图 19　细粒沉积岩中惰质体特征

（a）顺层状排列的惰质组丝质体，威远地区，X3 井，龙一 $_1$，2 653.40 m，MAPS 扫描图像，250 nm 分辨率[258]；（b）顺层分布的惰质组丝质体纵断面，新疆芦草沟组，扫描电镜[259]；（c）顺层分布的惰质组丝质体纵断面，三塘湖盆地芦草沟组，扫描电镜[255]；（d）惰质组丝质体横断面，矿物后期充填细胞空腔，华北石炭二叠系，扫描电镜[258]

Fig. 19　Characteristics of inertinite in fine-grained sedimentary rocks

(a)lamellar arrangement of inertinite fibrous matter, in the Weiyuan area, X3 well, Long1, 2 653.40 m, MAPS scanning image, 250 nm resolution[258]; (b)laminar distribution of longitudinal section of inertinite fibrous matter, in the Lucaogou Formation of Xinjiang, SEM[259]; (c)laminar distribution of longitudinal section of inertinite fibrous matter, in the Lucaogou Formation of the Santanhu Basin, SEM[255]; (d)transverse section of inertinite fibrous matter, with minerals filling the cell cavities later, in the Carboniferous-Permian of North China, SEM[258]

类脂体是细粒沉积岩中最常见的显微组分，其物质来源复杂，既包含来源于陆源的高等植物的孢子体、角质体、树脂体；也包含来源于盆内的浮游藻类、低等植物在厌氧菌的参与下形成的藻类体、沥青质体（无定形体）以及类脂碎屑体[28]。孢子体能够保存孢子以及花粉的形态特征，扫描电镜下常见的是呈扁平状、线状、蠕虫状、环状的小孢子（图 20a）[28]；角质体是由植物表皮的角质层形成的显微有机组分，表现出较强的韧性，常呈弯曲状、条带状分布在细粒沉积岩中（图 20b，c）[260]；树脂体是植物分泌物所形成的显微有机组分，常呈椭圆形、圆形分布在细粒沉积岩中，其表面平坦、轮廓清晰（图 20d）[261]。藻类体可划分为单个藻类体和层状藻类体，单个藻类体常呈无定形状、无定形团块状与细粒沉积矿物基质伴生（图 20e）[262]，层状藻类体在细粒沉积岩中常呈纹层状、条带状分布（图 20f）[28,261,263-264]；沥青质体来自被降解的藻类、细菌以及浮游植物[263-266]，没有固定形态，自然断面样品上常见其表面光滑平坦（图 20g），但在放大倍数的情况下可见沥青质内部的球粒结构（图 20h）[259]。

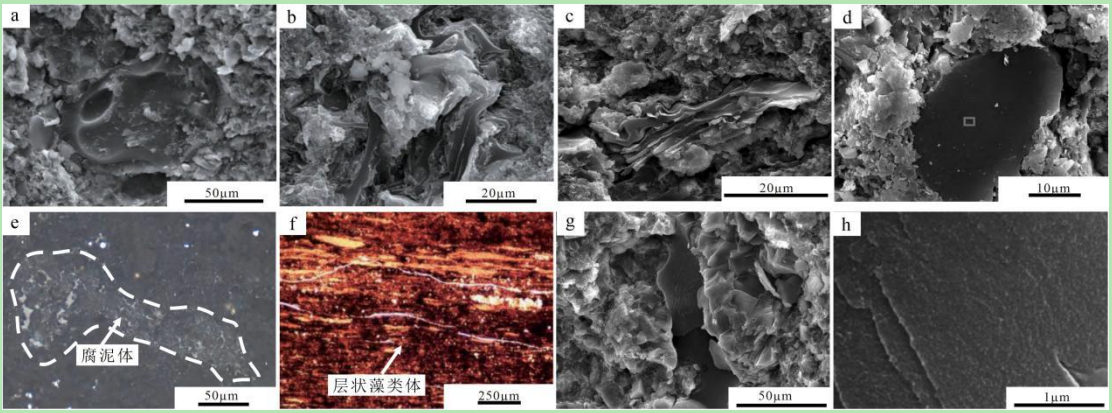

图 20　细粒沉积岩中类脂体特征

（a）切面呈圆环的孢子体，三塘湖盆地芦草沟组，扫描电镜[255]；（b）弯曲状角质体，三塘湖盆地芦草沟组，扫描电镜[255]；（c）层状角质体，新疆芦草沟组，扫描电镜[259]；（d）椭圆形树脂体，轮廓清晰，华北石炭二叠系，扫描电镜[259]；（e）单个无定形状藻类体，还保存着一定的藻类轮廓，内部由细小的有机质与黏土矿物组成，四川盆地五峰组—龙马溪组[262]；（f）呈条带状分布的层状藻类体，四川盆地渝西地区，Z202 井，龙马溪组，3 877.09 m，单偏光[263]；（g）条状沥青质，自然断面光滑平坦，新疆芦草沟组，扫描电镜[259]；（h）图 g 的局部放大,可见沥青质内部的球粒结构，新疆芦草沟组，扫描电镜[259]

Fig. 20　Characteristics of liptinite in fine-grained sedimentary rocks

(a)sporinite with a cross-section in the shape of a ring, in the Lucaogou Formation of the Santanhu Basin, SEM[255]; (b)curvilinear cutinite, in the Lucaogou Formation of the Santanhu Basin, SEM[255]; (c)lamellar cutinite, in the Lucaogou Formation of Xinjiang, SEM [259]; (d)oval resinite, with clear contours, in the Carboniferous-Permian of North China, SEM[259]; (e)individual amorphous alginite, still retaining a certain outline of algae, composed of fine organic matter and clay minerals inside, in the Wufeng Formation-Longmaxi Formation of the Sichuan Basin[262]; (f)lamellar alginite distributed in bands, in the Yuxi area of the Sichuan Basin, Z202 well, Longmaxi Formation, 3 877.09 m, PPL[263]; (g)strip-like bitumen, with a smooth and flat natural fracture, in the Lucaogou Formation of Xinjiang, SEM[259]; (h)a local magnification of Figure g, showing the granular structure inside the bitumen, in the Lucaogou Formation of Xinjiang, SEM[259]

动物有机碎屑常多来源于盆内，以笔石、几丁虫、牙形刺、有孔虫、苔藓虫等生物有机碎屑存在于细粒沉积岩中[250]，尤其是古生界细粒沉积岩地层中[266]，保存完好的动物有机碎屑能够较好地反映生物的形态和内部结构（图 21a~d）[259,267]。

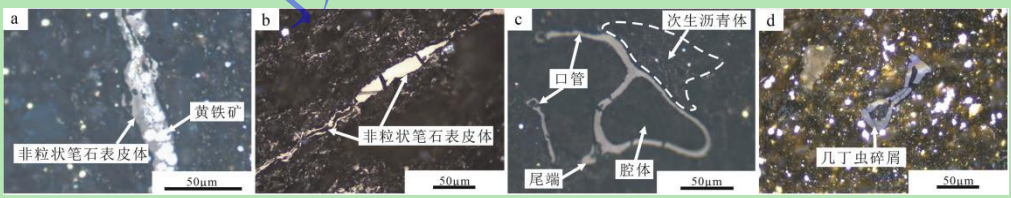

图 21　细粒沉积岩中动物有机碎屑特征

（a）非粒状笔石有机碎屑，笔石内部腔体被黄铁矿化，发育大量草莓状黄铁矿，四川盆地五峰组—龙马溪组[263]；（b）非粒状笔石有机体，中国重庆市巫溪县志留纪龙马溪组露头样品[252]；（c）几丁虫有机碎屑，墙体、口管、尾端形态完整，四川盆地五峰组—龙马溪组[262]；（d）几丁虫有机碎屑，美国 Illinois 盆地 New Albany 页岩[252]

Fig. 21　Characteristics of zooclastic organic debris in fine-grained sedimentary rocks

(a)non-granular graptolite organic debris, with the internal cavity of the graptolite mineralized by pyritization, developing a large number of strawberry-like pyrite, in the Wufeng Formation-Longmaxi Formation of the Sichuan Basin[263]; (b)non-granular graptolite organic matter, Outcrop samples from the Silurian Longmaxi Formation in Wuxi County, Chongqing, China[252]; (c)chitinozoan organic debris, with complete morphology of the wall, oral tube, and tail end, in the Wufeng Formation-Longmaxi Formation of the Sichuan Basin[262]; (d)chitinozoan organic debris, in the New Albany Shale of the Illinois Basin, USA[252]

次生有机质主要以固体沥青、焦沥青、微粒化沥青等形式存在于古生界及前寒武系细粒沉积岩中[253,268-269]。其成因复杂、种类多样[270]，但可以明确的是次生有机质与类脂体中的沥青质体物源相同，均来自盆内的水生浮游生物以及藻类等[259]。按照沥青和油气生成的先后关系可将生油前形成的沥青定义为油前沥青，如类脂体中的沥青质体，而次生有机质则是生油后形成的油后沥青[27,253]。次生有机质没有固定的形状（图 22a），部分展现出粒状镶嵌结构，具有明显的各向异性（图 22b）[269]。另外，次生沥青内部常发育经过改造作用后形成的纳米级圆形、椭圆形气孔（图 22c，d）[259]。

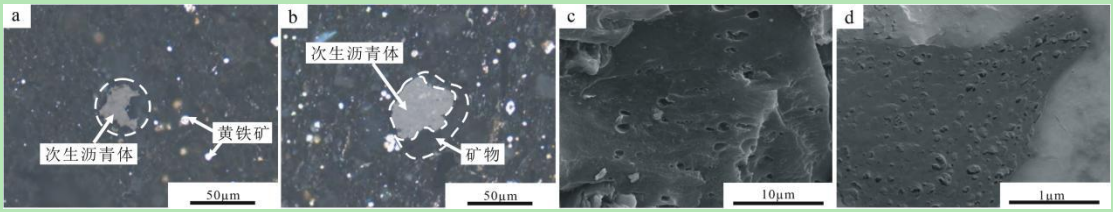

图 22　细粒沉积岩中次生有机质特征

（a）次生有机质沥青体，呈无定形状，四川盆地五峰组—龙马溪组[262]；（b）次生有机质沥青体，可见沥青呈团块状镶嵌在矿物中，四川盆地五峰组—龙马溪组[262]；（c）次生有机质沥青体，可见圆形、椭圆形气孔发育，南方下寒武统[259]；（d）次生有机质沥青体，可见抛光面上气泡状孔隙发育，南方下寒武统[259]

Fig. 22　Characteristics of secondary organic matter in fine-grained sedimentary rock

(a)secondary organic matter bitumen, amorphous, in the Wufeng Formation-Longmaxi Formation of the Sichuan Basin[262]; (b)secondary organic matter bitumen, visible bitumen inlaid in minerals in lumps, in the Wufeng Formation-Longmaxi Formation of the Sichuan Basin[262]; (c)secondary organic matter bitumen, well-developed circular and elliptical vesicles are visible, in the Lower Cambrian of the South[259]; (d)secondary organic matter bitumen, well-developed bubble-like pores are visible on the polished surface, Lower Cambrian, South China, in the Lower Cambrian of the South[259]

3　展望与结论

3.1　展望

近年来细粒沉积岩的相关研究已经取得显著进展，但整体依旧处于探索阶段。纵观细粒沉积岩的物源研究，多是局限于某些特定区域，而缺乏全球范围内的整体性系统研究，导致细粒沉积岩仍缺乏普遍适用的研究方法。在研究细粒沉积岩物质来源时，依旧以传统方法为主，如：野外剖面观测、岩心观察、薄片分析、X 射线衍射、地球化学分析、同位素分析等，这些方法虽然有效，但在处理复杂的物源问题时难免显得局限。

另外，目前细粒沉积岩的物源研究仍缺乏具有针对性的系统研究方案，多数学者在面对细粒沉积岩物源问题时仍采取传统粗粒度碎屑岩的部分方案，如：岩石矿物三段元法、重矿学方法、地质年代学方法、沉积相分析法、地球化学方法、地质年代学方法等，这些方法在一定程度上有效，但应对细粒沉积岩这样粒度较小、观察难度较大、物源多样的复杂物源分析时难免捉襟见肘。例如，由于细粒沉积岩物质组成粒度较细，难以与传统物源研究方法匹

配；对于多物源的细粒沉积岩利用传统物源研究方案，出现统计工作量大且难以达到准确溯源效果的弊端；传统物源研究手段应用到细粒沉积岩中容易出现成本较高、未考虑化学风化、搬运方式、迁移距离、沉积再分选等影响的缺陷。因此，细粒沉积岩物源研究的发展应集中在以下几个方面：

（1）在细粒沉积岩物质来源的研究中注重多学科的研究方法，如地质学、地球化学、地球物理学、水文学、微生物学、分子生物学等学科研究，以及新技术的应用，如数值模拟、化学模拟、水模拟、生物模拟等手段，以更加精确、直观了解不同细粒沉积物在“源—汇”系统中的迁移、转化和最终形成的微观形态和动态行为，同时更加全面地理解细粒沉积物在生物参与、不同的物理化学条件下的物理、化学和生物的成因机制。例如，利用水模拟、物理模拟、数值模拟等手段，模拟多种陆源碎屑沉积物质在侵蚀、搬运过程中的变化特征，深入探讨陆源细粒沉积物质在“源—汇”系统中的演化规律；通过研究细粒沉积物中的微生物群落的结构和功能，深入研究微生物在细粒沉积物尤其是黏土矿物、碳酸盐矿物的形成中起到的作用；利用先进技术手段，探究地球外部圈层和内部圈层如何控制陆源、内源、火山—热液源物质的耦合关系，进而控制富有机质细粒沉积岩的演化。

（2）深入研究细粒沉积岩对古环境的响应，例如，基于“源—汇”系统理论，利用铁、锂、钼等多种非传统同位素地球化学和XRF等技术，并辅以原型盆地恢复、岩相古地理重建等工作，明确古气候、古水深、古物源等环境变化如何控制细粒沉积物的发育和展布等。

（3）加强“将近论古”这一地质学中重要的思维方法在细粒沉积岩物质来源及物质成因方面的应用，通过现代细粒沉积物物质来源及沉积过程的研究，反演古代细粒沉积岩的物质来源及沉积过程。例如，研究现代沉积环境中细粒沉积物的物源、类型及分布，解释古代相似的沉积环境下细粒沉积物物源及物质成因的可能等。

（4）结合多种物源研究手段，在大量细粒沉积岩物源研究的基础上，对全球范围内的细粒沉积岩物源特征进行系统的归纳和总结，针对细粒沉积岩物质成分粒度较小、观察难度较大、物源复杂多样的特点，形成一套具有针对性、普遍适配性的细粒沉积岩物质来源研究方案，弥补目前细粒沉积岩缺乏统一的物源研究方案这一空缺。

通过以上方向的深入探索，我们有望从多角度揭示更加细致的细粒沉积岩物质来源方向，增强对细粒沉积岩形成机制的理解，推动细粒沉积学基础理论以及实际应用的发展。

3.2 结论

（1）陆源细粒沉积物是陆源区母岩经过风化作用形成的风化产物，经过河流、大气、冰川、生物等搬运介质搬运并进一步风化，最终沉积到盆地中形成的细粒沉积物质；内源细

粒沉积物是盆内生物—化学作用、化学作用、再搬运沉积作用以及生物作用形成的细粒物质；火山—热液细粒沉积物是火山喷发产生火山灰、火山尘形成的火山碎屑细粒沉积物质和通过断层或热液喷口输送到湖泊或海洋的上溢热液形成的热液细粒沉积物质。

（2）细粒沉积岩物质成分相当复杂，常见的有黏土矿物、石英、长石、碳酸盐矿物、黄铁矿、有机质等。黏土矿物为陆源成因、成岩作用黏土矿物转化成因、其他矿物溶蚀成因和海底火山物质溶解以及胞外聚合物生物介导作用形成；石英不仅可以来自陆源物质风化，也能来自盆内生物作用、火山喷发带来的凝灰物质经过脱玻化作用以及成岩自生作用形成；长石大部分来源于陆源碎屑物质风化，也可以由火山—热液作用提供，近年来相关研究也证实长石能够由微生物化学作用形成；碳酸盐矿物多为内源物质，受到盆内生物数量、陆源碎屑以及离子的供给、火山—热液微量元素的输入等多方面共同控制形成；黄铁矿中的铁和硫两大成矿元素来源复杂，河流输入、大气输入、冰川融解、盆内沉积物质再循环以及火山—热液均是铁元素和硫元素的来源，铁和硫在盆内经过异化铁还原和铁穿梭机制还原以及MSR 和 TSR 作用形成黄铁矿；细粒沉积岩中的有机质类型复杂多样，可划分为陆源的镜质体、惰质体和部分类脂体以及内源的部分类脂体、动物有机碎屑和次生有机质。

（3）目前细粒沉积岩物源研究方法常采用传统粗粒度碎屑岩物源分析方法，缺乏具有针对性的细粒沉积岩物源分析方案。未来细粒沉积岩的物源研究将围绕多学科、高精度等方面发展，而当下仍亟待一套适用于细粒沉积岩物源研究的系统方案形成。

参考文献（References）

[1] 贾承造. 中国石油工业上游前景与未来理论技术五大挑战[J]. 石油学报，2024，45（1）：1-14. [Jia Chengzao. Prospects and five future theoretical and technical challenges of the upstream petroleum industry in China[J]. Acta Petrolei Sinica, 2024, 45(1): 1-14.]

[2] 邹才能，杨智，张国生，等. 非常规油气地质学理论技术及实践[J]. 地球科学，2023，48（6）：2376-2397. [Zou Caineng, Yang Zhi, Zhang Guosheng, et al. Theory, technology and practice of unconventional petroleum geology[J]. Earth Science, 2023, 48(6): 2376-2397.]

[3] 朱如凯，孙龙德，张天舒，等. 中国油气勘探开发中的沉积学研究新进展与发展方向[J/OL]. 沉积学报. https://doi.org/10.14027/j.issn.1000-0550.2024.075. [Zhu Rukai, Sun Longde, Zhang Tianshu, et al. Advances and trends in sedimentological research in oil and gas exploration and development in China[J/OL]. Acta Sedimentologica Sinica. https://doi.org/10.14027/j.issn.1000-0550.2024.075.]

[4] Aplin A C, Macquaker J H S. Mudstone diversity: Origin and implications for source, seal, and reservoir properties in petroleum systems[J]. AAPG Bulletin, 2011, 95(12): 2031-2059.

[5] 姜在兴，梁超，吴靖，等. 含油气细粒沉积岩研究的几个问题[J]. 石油学报，2013，34（6）：1031-1039. [Jiang Zaixing, Liang Chao, Wu Jing, et al. Several issues in sedimentological studies on hydrocarbon-bearing fine-grained sedimentary rocks[J]. Acta Petrolei Sinica, 2013, 34(6): 1031-1039.]

[6] Dittrich M, Müller B, Mavrocordatos D, et al. Induced calcite precipitation by cyanobacterium *Synechococcus*[J]. Acta Hydrochimica et Hydrobiologica, 2003, 31(2): 162-169.

[7] Shen Y, Suarez-Gonzalez P, Reitner J. Contrasting modes of carbonate precipitation in a hypersaline microbial mat and their influence on biomarker preservation (kiritimati, central pacific)[J]. Minerals, 2022, 12(2): 267.

[8] Valero Garcés B L. Lacustrine deposition and related volcanism in a transtensional tectonic setting: Upper Stephanian-Lower Autunian in the Aragón-Béarn Basin, western Pyrenees (Spain-France)[J]. Sedimentary Geology, 1993, 83(1/2): 133-160.

[9] 郭佩，李长志，文华国，等. 陆相硅质岩成因类型及构造—气候指示意义[J]. 沉积学报，2022，40（2）：450-464. [Guo Pei, Li Changzhi, Wen Huaguo, et al. Genesis of continental siliceous rocks and their tectonic-climatic significance[J]. Acta Sedimentologica Sinica, 2022, 40(2): 450-464.]

[10] 柳益群，周鼎武，焦鑫，等. 深源物质参与湖相烃源岩生烃作用的初步研究：以准噶尔盆地吉木萨尔凹陷二叠系黑色岩系为例[J]. 古地理学报，2019，21（6）：983-998. [Liu Yiqun, Zhou Dingwu, Jiao Xin, et al. A preliminary study on the relationship between deep-sourced materials and hydrocarbon generation in lacustrine source rocks: An example from the Permian black rock series in Jimusar Sag, Junggar Basin[J]. Journal of Palaeogeography (Chinese Edition), 2019, 21(6): 983-998.]

[11] 南云. 新疆北东部三塘湖地区晚石炭世—二叠纪岩浆活动及成盆构造背景研究[D]. 西安：西北大学，2018. [Nan Yun. Magmatic activity and tectonic setting of Basin Formation from Late Carboniferous to Permian in Santanghu area, NE Xinjiang[D]. Xi'an: Northwest University, 2018.]

[12] Zou C N, Zhu R K, Chen Z Q, et al. Organic-matter-rich shales of China[J]. Earth-Science Reviews, 2019, 189: 51-78.

[13] Arthur M A, Sageman B B. MARINE BLACK SHALES: Depositional mechanisms and environments of ancient deposits[J]. Annual Review of Earth and Planetary Sciences, 1994, 22: 499-551.

[14] 张鸿禹，杨文涛. 陆相细粒沉积岩与古土壤深时气候分析方法综述[J]. 沉积学报，2023，41（2）：333-348. [Zhang Hongyu, Yang Wentao. Research status of deep-time paleoclimate analysis methods for terrestrial pulveryte and paleosols[J]. Acta Sedimentologica Sinica, 2023, 41(2): 333-348.]

[15] Wang W W, Jiang Z X, Xie X Y, et al. Sedimentary characteristics and interactions among volcanic, terrigenous and marine processes in the Late Permian Kuishan member, eastern Block of the North China Craton[J]. Sedimentary Geology, 2020, 407: 105741.

[16] Liang C, Cao Y C, Liu K Y, et al. Diagenetic variation at the lamina scale in lacustrine organic-rich shales: Implications for hydrocarbon migration and accumulation[J]. Geochimica et Cosmochimica Acta, 2018, 229: 112-128.

[17] 黎茂稳，马晓潇，金之钧，等. 中国海、陆相页岩层系岩相组合多样性与非常规油气勘探意义[J]. 石油与天然气地质，2022，43（1）：1-25. [Li Maowen, Ma Xiaoxiao, Jin Zhijun, et al. Diversity in the lithofacies assemblages of marine and lacustrine shale strata and significance for unconventional petroleum exploration in China[J]. Oil & Natural Gas Geology, 2022, 43(1): 1-25.]

[18] 朱红涛，徐长贵，朱筱敏，等. 陆相盆地源—汇系统要素耦合研究进展[J]. 地球科学，2017，42（11）：1851-1870. [Zhu Hongtao, Xu Changgui, Zhu Xiaomin, et al. Advances of the source-to-sink units and coupling model research in continental Basin[J]. Earth Science, 2017, 42(11): 1851-1870.]

[19] 路畅，夏国清，陈云，等. 西藏伦坡拉盆地晚始新世—早渐新世黏土矿物特征及古气候意义[J]. 沉积与特提斯地质，2023，43（3）：565-579. [Lu Chang, Xia Guoqing, Chen Yun, et al. Late Eocene-Early Oligocene clay mineral characteristics and paleoclimate significance in Lunpola Basin, Tibet[J]. Sedimentary Geology and Tethyan Geology, 2023, 43(3): 565-579.]

[20] 易婷. 川南五峰组—龙马溪组富有机质页岩硅质特征与储层之间的关系[D]. 成都：成都理工大学，2020. [Yi Ting. Relationship between silica's characteristics and reservoirs of the organic-rich shale in Wufeng Formation-Longmaxi Formation in southern Sichuan Basin[D]. Chengdu: Chengdu University of Technology, 2020.]

[21] 赵迪斐. 川东下古生界五峰组—龙马溪组页岩储层孔隙结构精细表征[D]. 徐州：中国矿业大学，2021. [Zhao Difei. Quantitative characterization of pore structure of shale reservoirs in the Lower Paleozoic Wufeng-Longmaxi Formation of the East Sichuan area[D]. Xuzhou: China University of Mining and Technology, 2021.]

[22] 江新胜，徐金沙，潘忠习. 鄂尔多斯盆地白垩纪沙漠石英沙颗粒表面特征[J]. 沉积学报，2003，21（3）：416-422. [Jiang Xinsheng, Xu Jinsha, Pan Zhongxi. Microscopic features on quartz sand grain surface in the Cretaceous desert of Ordos Basin[J]. Acta Sedimentologica Sinica, 2003, 21(3): 416-422.]

[23] 汤海磊. 楚雄盆地东北部白垩纪风成沉积特征与古气候研究[D]. 成都：成都理工大学，2020. [Tang Hailai. Sedimentary characteristics and palaeoclimatic implications of the Cretaceous Aeolian erg system in the northeastern Chuxiong Basin, China[D]. Chengdu: Chengdu University of Technology, 2020.]

[24] Zheng L J, Jiang Z X, Liu H, et al. Core evidence of paleoseismic events in Paleogene deposits of the Shulu Sag in the Bohai Bay Basin, east China, and their petroleum geologic significance[J]. Sedimentary Geology, 2015, 328: 33-54.

[25] 任韵清. 用微古植物群探讨束鹿凹陷的沉积环境[J]. 沉积学报，1986，4（4）：101-107. [Ren Yunqing. Depositional environments of Shulu Depression: Viewed from the point of micropaleobotanic florae[J]. Acta Sedimentologica Sinica, 1986, 4(4): 101-107.]

[26] Jiang Z X, Chen D Z, Qiu L W, et al. Source-controlled carbonates in a small Eocene half-graben lake Basin (Shulu Sag) in central Hebei province, North China[J]. Sedimentology, 2007, 54(2): 265-292.

[27] Mastalerz M, Drobniak A, Stankiewicz A B. Origin, properties, and implications of solid bitumen in source-rock reservoirs: A review[J]. International Journal of Coal Geology, 2018, 195: 14-36.

[28] 代世峰，赵蕾，唐跃刚，等. 煤的显微组分定义与分类（ICCP system 1994）解析Ⅳ：类脂体[J]. 煤炭学报，2021，46（9）：2965-2983. [Dai Shifeng, Zhao Lei, Tang Yuegang, et al. An in-depth interpretation of definition and classification of macerals in coal (ICCP system 1994) for Chinese researchers, IV: Liptinite[J]. Journal of China Coal Society, 2021, 46(9): 2965-2983.]

[29] 姜在兴，孔祥鑫，杨叶芃，等. 陆相碳酸盐质细粒沉积岩及油气甜点多源成因[J]. 石油勘探与开发，2021，48（1）：26-37. [Jiang Zaixing, Kong Xiangxin, Yang Yepeng, et al. Multi-source genesis of continental carbonate-rich fine-grained sedimentary rocks and hydrocarbon sweet spots[J]. Petroleum Exploration and Development, 2021, 48(1): 26-37.]

[30] 蒋宜勤，柳益群，杨召，等. 准噶尔盆地吉木萨尔凹陷凝灰岩型致密油特征与成因[J]. 石油勘探与开发，2015，426）：741-749. [Jiang Yiqin, Liu Yiqun, Yang Zhao, et al. Characteristics and origin of tuff-type tight oil in Jimusar Depression, Junggar Basin, NW China[J]. Petroleum Exploration and Development, 2015, 42(6): 741-749.]

[31] 姜在兴，王运增，王力，等. 陆相细粒沉积岩物质来源、搬运—沉积机制及多源油气甜点[J]. 石油与天然气地质，2022，43（5）：1039-1048. [Jiang Zaixing, Wang Yunzeng, Wang Li, et al. Review on provenance, transport-sedimentation dynamics and multi-source hydrocarbon sweet spots of continental fine-grained sedimentary rocks[J]. Oil & Natural Gas Geology, 2022, 43(5): 1039-1048.]

[32] 孔祥鑫. 湖相含碳酸盐细粒沉积岩特征、成因与油气聚集[D]. 北京：中国地质大学（北京），2020. [Kong Xiangxin. Sedimentary characteristics, origin and hydrocarbon accumulation of lacustrine carbonate-bearing fine-grained sedimentary rocks[D]. Beijing: China University of Geosciences (Beijing), 2020.]

[33] Gierlowski-Kordesch E H. Lacustrine carbonates[J]. Developments in Sedimentology, 2010, 61: 1-101.

[34] Liang C, Jiang Z X, Cao Y C, et al. Sedimentary characteristics and origin of lacustrine organic-rich shales in the salinized Eocene Dongying Depression[J]. GSA Bulletin, 2018, 130(1/2): 154-174.

[35] 操应长，梁超，韩豫，等. 基于物质来源及成因的细粒沉积岩分类方案探讨[J]. 古地理学报，2023，25（4）：729-741. [Cao Yingchang, Liang Chao, Han Yu, et al. Discussions on classification scheme for fine-grained sedimentary rocks based on sediments sources and genesis[J]. Journal of Palaeogeography (Chinese Edition), 2023, 25(4): 729-741.]

[36] 姜在兴，张建国，孔祥鑫，等. 中国陆相页岩油气沉积储层研究进展及发展方向[J]. 石油学报，2023，44（1）：45-71. [Jiang Zaixing, Zhang Jianguo, Kong Xiangxin, et al. Research progress and development direction of continental shale oil and gas deposition and reservoirs in China[J]. Acta Petrolei Sinica, 2023, 44(1): 45-71.]

[37] Dittrich M, Obst M. Are picoplankton responsible for calcite precipitation in lakes?[J]. AMBIO: A Journal of the Human Environment, 2004, 33(8): 559-564.

[38] Schimmelmann A, Lange C B, Schieber J, et al. Varves in marine sediments: A review[J]. Earth-Science Reviews, 2016, 159: 215-246.

[39] 郭旭升，李宇平，腾格尔，等. 四川盆地五峰组—龙马溪组深水陆棚相页岩生储机理探讨[J]. 石油勘探与开发，2020，47（1）：193-201. [Guo Xusheng, Li Yuping, Borjigen T, et al. Hydrocarbon generation and storage mechanisms of deep-water shelf shales of Ordovician Wufeng Formation–Silurian Longmaxi Formation in Sichuan Basin, China[J]. Petroleum Exploration and Development, 2020, 47(1): 193-201.]

[40] Gao P, He Z L, Lash G G, et al. Controls on silica enrichment of Lower Cambrian organic-rich shale deposits[J]. Marine and Petroleum Geology, 2021, 130: 105126.

[41] 陈斐然，刘珠江，陆永潮，等. 川东北地区中—上二叠统层序地层格架内多重地质事件耦合的富有机质页岩成因模式[J]. 地

球科学进展，2024，39（5）：519-531. [Chen Feiran, Liu Zhujiang, Lu Yongchao, et al. Organic-rich shale genesis model coupled with multiple geological events in Middle-Upper Permian sequence stratigraphic framework in northeastern Sichuan[J]. Advances in Earth Science, 2024, 39(5): 519-531.]

[42] 孙龙德，王凤兰，白雪峰，等. 页岩中纳米级有机黏土复合孔缝的发现及其科学意义：以松辽盆地白垩系青山口组页岩为例[J]. 石油勘探与开发，2024，51（4）：708-719，758. [Sun Longde, Wang Fenglan, Bai Xuefeng, et al. Discovery of nano organo-clay complex pore-fractures in shale and its scientific significances: A case study of Cretaceous Qingshankou Formation shale, Songliao Basin, NE China[J]. Petroleum Exploration and Development, 2024, 51(4): 708-719, 758.]

[43] Delmelle P, Lambert M, Dufrêne Y, et al. Gas/aerosol–ash interaction in volcanic plumes: New insights from surface analyses of fine ash particles[J]. Earth and Planetary Science Letters, 2007, 259(1/2): 159-170.

[44] 张文正，杨华，彭平安，等. 晚三叠世火山活动对鄂尔多斯盆地长 7 优质烃源岩发育的影响[J]. 地球化学，2009，38（6）：573-582. [Zhang Wenzheng, Yang Hua, Peng Ping'an, et al. The Influence of Late Triassic volcanism on the development of Chang 7 high grade hydrocarbon source rock in Ordos Basin[J]. Geochemistry, 2009, 38(6): 573-582.]

[45] 王书荣，宋到福，何登发. 三塘湖盆地火山灰对沉积有机质的富集效应及凝灰质烃源岩发育模式[J]. 石油学报，2013，34（6）：1077-1087. [Wang Shurong, Song Daofu, He Dengfa. The enrichment effect of volcanic ash on sedimentary organic matter and the development pattern of tuffaceous hydrocarbon source rocks in the Santanhu Basin[J]. Acta Petrolei Sinica, 2013, 34(6): 1077-1087.]

[46] Zhang W Z, Yang W W, Xie L Q. Controls on organic matter accumulation in the Triassic Chang 7 lacustrine shale of the Ordos Basin, central China[J]. International Journal of Coal Geology, 2017, 183: 38-51.

[47] 李森，朱如凯，崔景伟，等. 鄂尔多斯盆地长 7 段细粒沉积岩特征与古环境：以铜川地区瑶页 1 井为例[J]. 沉积学报，2020，38（3）：554-570. [Li Sen, Zhu Rukai, Cui Jingwei, et al. Sedimentary Characteristics of Fine-grained Sedimentary Rock and Paleo-environment of Chang 7 member in the Ordos Basin: A case study from Well Yaoye 1 in Tongchuan[J]. Acta Sedimentologica Sinica, 2020, 38(3): 554-570.]

[48] Shearme S, Cronan D S, Rona P A. Geochemistry of sediments from the TAG Hydrothermal Field, M.A.R. at latitude 26° N[J]. Marine Geology, 1983, 51(3/4): 269-291.

[49] Jiao X, Liu Y Q, Yang W, et al. A magmatic-hydrothermal lacustrine exhalite from the Permian Lucaogou Formation, Santanghu Basin, NW China - The volcanogenic origin of fine-grained clastic sedimentary rocks[J]. Journal of Asian Earth Sciences, 2018, 156: 11-25.

[50] 柳益群，周鼎武，焦鑫，等. 一类新型沉积岩：地幔热液喷积岩：以中国新疆三塘湖地区为例[J]. 沉积学报，2013，31（5）：773-781. [Liu Yiqun, Zhou Dingwu, Jiao Xin, et al. A new type of sedimentary rocks: Mantle-originated hydroclastites and hydrothermal exhalites, Santanghu area, Xinjiang, NW China[J]. Acta Sedimentologica Sinica, 2013, 31(5): 773-781.]

[51] 郑庆华，刘行军，柳益群，等. 鄂尔多斯盆地延长组长 7 油层组碳酸质喷积岩初探[J]. 沉积学报，2021，39（5）：1222-1238. [Zheng Qinghua, Liu Xingjun, Liu Yiqun, et al. A preliminary study of carbonatite magmatic-hydrothermal exhalative sedimentary rock of the Chang 7 member, Yanchang Formation, Ordos Basin[J]. Acta Sedimentologica Sinica, 2021, 39(5): 1222-1238.]

[52] 焦鑫，柳益群，周鼎武，等. 湖相烃源岩中的火山—热液深源物质与油气生成耦合关系研究进展[J]. 古地理学报，2021，23（4）：789-809. [Jiao Xin, Liu Yiqun, Zhou Dingwu, et al. Progress on coupling relationship between volcanic and hydrothermal-originated sediments and hydrocarbon generation in lacustrine source rocks[J]. Journal of Palaeogeography (Chinese Edition), 2021, 23(4): 789-809.]

[53] Edmond J M, Von Damm K L, McDuff R E, et al. Chemistry of hot springs on the East Pacific Rise and their effluent dispersal[J]. Nature, 1982, 297(5863): 187-191.

[54] 陈先沛，高计元，陈多福，等. 热水沉积作用的概念和几个岩石学标志[J]. 沉积学报，1992，10（3）：124-132. [Chen Xianpei, Gao Jiyuan, Chen Duofu, et al. The concept of hydrothermal sedimentation and its petrological criteria[J]. Acta Sedimentologica Sinica, 1992, 10(3): 124-132.]

[55] 王江海. 陆相热水沉积的地质地球化学判别标志研究[J]. 矿物岩石地球化学通讯，1993（2）：68-69. [Wang Jianghai. Study on the Geological and Geochemical Discriminative Indicators of Continental Hydrothermal Sedimentation[J]. Bulletin of Mineralogy,

Petrology and Geochemistry, 1993(2): 68-69.]

[56] 常海亮，郑荣才，郭春利，等. 准噶尔盆地西北缘风城组喷流岩稀土元素地球化学特征[J]. 地质论评，2016，62（3）：550-568. [Chang Hailiang, Zheng Rongcai, Guo Chunli, et al. Characteristics of rare earth elements of exhalative rock in Fengcheng Formation, Northwestern Margin of Jungger Basin[J]. Geological Review, 2016, 62(3): 550-568.]

[57] 贾斌，文华国，李颖博，等. 准噶尔盆地乌尔禾地区二叠系风城组盐类矿物流体包裹体特征[J]. 沉积与特提斯地质，2015，35（1）：33-42. [Jia Bin, Wen Huaguo, Li Yingbo, et al. Fluid inclusions in the salt minerals from the Permian Fengcheng Formation in the Urho region, Junggar Basin, Xinjiang[J]. Sedimentary Geology and Tethyan Geology, 2015, 35(1): 33-42.]

[58] 焦鑫，柳益群，杨晚，等. 水下火山喷发沉积特征研究进展[J]. 地球科学进展，2017，32（9）：926-936. [Jiao Xin, Liu Yiqun, Yang Wan, et al. Progress on sedimentation of subaqueous volcanic eruption[J]. Advances in Earth Science, 2017, 32(9): 926-936.]

[59] 柳益群，焦鑫，李红，等. 新疆三塘湖跃进沟二叠系地幔热液喷流型原生白云岩[J]. 中国科学（D 辑）：地球科学，2011，41（12）：1862-1871. [Liu Yiqun, Jiao Xin, Li Hong, et al. Primary Dolostone Formation related to mantle-originated exhalative hydrothermal activities, Permian Yuejingou Section, Santanghu area, Xinjiang, NW China[J]. Science China (Seri. D): Earth Sciences, 2011, 41(12): 1862-1871.]

[60] 贺聪，吉利明，苏奥，等. 鄂尔多斯盆地南部延长组热水沉积作用与烃源岩发育的关系[J]. 地学前缘，2017，24（6）：277-285. [He Cong, Ji Liming, Su Ao, et al. Relationship between hydrothermal sedimentation process and source rock development in the Yanchang Formation in southern Ordos Basin[J]. Earth Science Frontiers, 2017, 24(6): 277-285.]

[61] He C, Ji L M, Wu Y D, et al. Characteristics of hydrothermal sedimentation process in the Yanchang Formation, south Ordos Basin, China: Evidence from element geochemistry[J]. Sedimentary Geology, 2016, 345: 33-41.

[62] 郑荣才，文华国，李云，等. 甘肃酒西盆地青西凹陷下白垩统下沟组湖相喷流岩物质组分与结构构造[J]. 古地理学报，2018，20（1）：1-18. [Zheng Rongcai, Wen Huaguo, Li Yun, et al. Compositions and texture of lacustrine exhalative rocks from the Lower Cretaceous Xiagou Formation in Qingxi Sag of Jiuxi Basin, Gansu[J]. Journal of Palaeogeography (Chinese Edition), 2018, 20(1): 1-18.]

[63] 李哲萱，柳益群，焦鑫，等. 湖相细粒沉积岩中的“斑状”深源碎屑：以准噶尔盆地吉木萨尔凹陷芦草沟组为例[J]. 天然气地球科学，2020，31（2）：220-234. [Li Zhexuan, Liu Yiqun, Jiao Xin, et al. Deep-derived clastics with porphyroclastic structure in lacustrine fine-grained sediments: Case study of the Permian Lucaogou Formation in Jimsar Sag, Junggar Basin[J]. Natural Gas Geoscience, 2020, 31(2): 220-234.]

[64] 杨娅敏，曾志刚，殷学博，等. 700 年以来冲绳海槽南部黏土矿物来源及其对沉积环境的响应[J]. 海洋科学，2021，45（11）：42-53. [Yang Yamin, Zeng Zhigang, Yin Xuebo, et al. Sediment provenance and its response to the paleoenvironment in the southern Okinawa Trough over the past 700 years[J]. Marine Sciences, 2021, 45(11): 42-53.]

[65] Biscaye P E. Mineralogy and sedimentation of recent deep-sea clay in the Atlantic ocean and adjacent seas and oceans[J]. GSA Bulletin, 1965, 76(7): 803-832.

[66] Dou Y G, Li J, Zhao J T, et al. Clay mineral distributions in surface sediments of the Liaodong Bay, Bohai Sea and surrounding river sediments: Sources and transport patterns[J]. Continental Shelf Research, 2014, 73: 72-82.

[67] 杨雅秀. 中国粘土矿物[M]. 北京：地质出版社，1994. [Yang Yaxiu. Clay minerals of China[M]. Beijing: Geological Publishing House, 1994.]

[68] 赵亚杰. 垦利 6 围区新近系火山岩岩相特征研究[D]. 北京：中国石油大学（北京），2016. [Zhao Yajie. Lithofacies characteristics of the Neogene volcanic strata in the Kenli 6 area[D]. Beijing: China University of Petroleum (Beijing), 2016.]

[69] 陆景冈. 土壤地质学[M]. 北京：地质出版社，1997. [Lu Jinggang. Geopedology[M]. Beijing: Geological Publishing House, 1997.]

[70] Chamley H. Clay sedimentation and paleoenvironment in the Shikoku Basin since the Middle Miocene (Deep Sea Drilling Project leg 58, North Philippine Sea)[J]. Initial reports of the Deep Sea Drilling Project, Leg 58, Yokohama, Japan to Okinawa, Japan, December 1977 - January 1978, 1980, 58: 669-681.

[71] 明洁. 东菲律宾海帕里西维拉海盆第四纪沉积特征和物质来源及其古环境意义[D]. 青岛：中国科学院研究生院（海洋研究所），2013. [Ming Jie. The characeristics and provenance of the sediment in the Parece Vela Basin since the Quaternary and their environmental implications[D]. Qingdao: University of Chinese Academy of Sciences (Institute of Oceanology), 2013.]

[72] Chamley H. Clay sedimentology[M]. Berlin, Heidelberg: Springer, 1989.

[73] Liu Z F, Zhao Y L, Colin C, et al. Source-to-sink transport processes of fluvial sediments in the South China Sea[J]. Earth-Science Reviews, 2016, 153: 238-273.

[74] de Segonzac G D. The transformation of clay minerals during diagenesis and low-grade metamorphism: A review[J]. Sedimentology, 1970, 15(3/4): 281-346.

[75] Sheldon N D, Tabor N J. Quantitative paleoenvironmental and paleoclimatic reconstruction using paleosols[J]. Earth-Science Reviews, 2009, 95(1/2): 1-52.

[76] Robert C. Late Quaternary variability of precipitation in southern California and climatic implications: Clay mineral evidence from the Santa Barbara Basin, ODP Site 893[J]. Quaternary Science Reviews, 2004, 23(9/10): 1029-1040.

[77] Jiménez-Espinosa R, Jiménez-Millán J. Calcrete development in mediterranean colluvial carbonate systems from SE Spain[J]. Journal of Arid Environments, 2003, 53(4): 479-489.

[78] 刘华华，蒋富清，周烨，等. 晚更新世以来奄美三角盆地黏土矿物的来源及其对古气候的指示[J]. 地球科学进展，2016，31（3）：286-297. [Liu Huahua, Jiang Fuqing, Zhou Ye, et al. Provenance of clay minerals in the amami sankaku Basin and their paleoclimate implications since Late Pleistocene[J]. Advances in Earth Science, 2016, 31(3): 286-297.]

[79] 王银，吕士辉，苏新，等. 西北太平洋多金属结核区沉积物黏土矿物特征[J]. 中国有色金属学报，2021，31（10）：2696-2712. [Wang Yin, Lü Shihui, Su Xin, et al. Assemblage of clay minerals at polymetallic nodules contract area in Northwest Pacific Ocean[J]. The Chinese Journal of Nonferrous Metals, 2021, 31(10): 2696-2712.]

[80] 汤艳杰，贾建业，谢先德. 粘土矿物的环境意义[J]. 地学前缘，2002，9（2）：337-344. [Tang Yanjie, Jia Jianye, Xie Xiande. Environment significance of clay minerals[J]. Earth Science Frontiers, 2002, 9(2): 337-344.]

[81] Berger G, Lacharpagne J C, Velde B, et al. Kinetic constraints on illitization reactions and the effects of organic diagenesis in sandstone/shale sequences[J]. Applied Geochemistry, 1997, 12(1): 23-35.

[82] 郇金来，黄思静，黄可可，等. 川西须二段碎屑岩钾长石钠长石化的热力学解释[J]. 断块油气田，2011，18（3）：289-292. [Huan Jinlai, Huang Sijing, Huang Keke, et al. Thermodynamics interpretation for albitization of detrital K-feldspar of T_3x^2 member in western Sichuan Depression[J]. Fault-Block Oil & Gas Field, 2011, 18(3): 289-292.]

[83] 王秀平，牟传龙，葛祥英，等. 四川盆地南部及其周缘龙马溪组黏土矿物研究[J]. 天然气地球科学，2014，25（11）：1781-1794. [Wang Xiuping, Mou Chuanlong, Ge Xiangying, et al. Study on clay minerals in the Lower Silurian Longmaxi Formation in southern Sichuan Basin and its periphery[J]. Natural Gas Geoscience, 2014, 25(11): 1781-1794.]

[84] Merriman R J. Clay minerals and sedimentary Basin history[J]. European Journal of Mineralogy, 2005, 17(1): 7-20.

[85] Jeong G Y, Yoon H I. The origin of clay minerals in soils of King George Island, South Shetland Islands, West Antarctica, and its implications for the clay-mineral compositions of marine sediments[J]. Journal of Sedimentary Research, 2001, 71(5): 833-842.

[86] 黄璞，熊亮，詹国卫，等. 基于米兰科维奇理论页岩岩相组合研究：以四川盆地南部龙马溪组一段为例[J/OL]. 沉积学报. https://doi.org/10.14027/j.issn.1000-0550.2023.119. [Huang Pu, Xiong Liang, Zhan Guowei, et al. Research on shale faciescombination based on milankovitch theory: A case study from the 1st member of Longmaxi Formation in the southern Sichuan Basin[J/OL]. Acta Sedimentologica Sinica. https://doi.org/10.14027/j.issn.1000-0550.2023.119.]

[87] 邓韬，许冬，肖婷露，等. 西太平洋海山盆地沉积物黏土矿物特征及其指示意义[J]. 海洋学研究，2023，41（3）：56-72. [Deng Tao, Xu Dong, Xiao Tinglu, et al. Clay mineral characteristics of sediments in the seamount Basin of the western Pacific and its indicative significance[J]. Journal of Marine Sciences, 2023, 41(3): 56-72.]

[88] 靳宁，李安春，刘海志，等. 帕里西维拉海盆西北部表层沉积物中粘土矿物的分布特征及物源分析[J]. 海洋与湖沼，2007，38（6）：504-511. [Jin Ning, Li Anchun, Liu Haizhi, et al. Clay minerals in surface sediment of the northwest parece vela Basin: Distribution and provenance[J]. Oceanologia et Limnologia Sinica, 2007, 38(6): 504-511.]

[89] Calvo J P, Blanc-Valleron M M, Rodríguez-Arandía J P, et al. Authigenic clay minerals in continental evaporitic environments[M]//Thiry M, Simon-Coinçon R. Palaeoweathering, palaeosurfaces and related continental deposits. Oxford: Blackwell Publishing Ltd., 1995: 51.

[90] Ueshima M, Tazaki K. Possible role of microbial polysaccharides in nontronite Formation[J]. Clays and Clay Minerals, 2001, 49(4):

292-299.

[91] Burne R V, Moore L S, Christy A G, et al. Stevensite in the modern thrombolites of Lake Clifton, western Australia: A missing link in microbialite mineralization?[J]. Geology, 2014, 42(7): 575-578.

[92] Zeyen N, Benzerara K, Li J H, et al. Formation of low-T hydrated silicates in modern microbialites from Mexico and implications for microbial fossilization[J]. Frontiers in Earth Science, 2015, 3: 64.

[93] 王杰，邵光辉，丁嘉. 微生物分解硅酸盐矿物增黏对砂土强度的影响[J]. 林业工程学报，2024，9（4）：154-161. [Wang Jie, Shao Guanghui, Ding Jia. Effects of clay content increasement by microbial decomposition of silicate minerals on the strength characteristics of sand[J]. Journal of Forestry Engineering, 2024, 9(4): 154-161.]

[94] Zhang N, Yan Y T, Li S R, et al. Combination distribution characteristics and corresponding material sources of surface clay minerals in Beibu Gulf, China[J]. Advanced Materials Research, 2012, 616-618: 158-161.

[95] Liu J Q, Liu Y L, Yin P, et al. Composition, source and environmental indication of clay minerals in sediments from mud deposits in he southern Weihai offshore, northwestern shelf of the South Yellow Sea, China[J]. Journal of Ocean University of China, 2022, 21(5): 1161-1173.

[96] Li J R, Liu S F, Shi X F, et al. Distributions of clay minerals in surface sediments of the Middle Bay of Bengal: Source and transport pattern[J]. Continental Shelf Research, 2017, 145: 59-67.

[97] Jadhav K P, Ahmed N, Datta S P, et al. Clay mineralogical diversity in soil systems: Insights from XRD analyses across diverse soil orders[J]. Clay Research, 2022, 41(2): 95-101.

[98] Zanoni G, Šegvić B, Sweet D E. Clay mineral diagenesis in alternating mudstone-sandstone beds from Late Palaeozoic strata of the Anadarko Basin, United States[J]. Geological Journal, 2023, 58(1): 108-130.

[99] Hu Q N, Yang B J, Liu J H, et al. Geochemical and mineral composition characteristics of hydrothermal-related clay-sized surface sediments from southern Mid-Atlantic Ridge: Implications for hydrothermal depositional environment[J]. Ore Geology Reviews, 2023, 162: 105674.

[100] 张会娜，管勇，窦衍光，等. 胶州湾表层沉积物黏土矿物分布特征及物源分析[J]. 海洋地质前沿，2023，39（8）：20-28. [Zhang Huina, Guan Yong, Dou Yanguang, et al. Clay mineral assemblages and provenance in the surface sediment of Jiaozhou Bay[J]. Marine Geology Frontiers, 2023, 39(8): 20-28.]

[101] Hu Q N, Li C S, Yang B J, et al. Clay mineral distribution characteristics of surface sediments in the South Mid-Atlantic Ridge[J]. Journal of Oceanology and Limnology, 2023, 41(3): 897-908.

[102] Chen M, Qi H S, Wasuwatcharapong A, et al. Clay mineral compositions in the surface sediment of the Chanthaburi coast (northeastern Gulf of Thailand) and their implications on sediment provenance[J]. Journal of Oceanology and Limnology, 2023, 41(5): 1742-1752.

[103] Chen Y Y, Li W J, Hou Z F, et al. Clay minerals and provenancial implications of surface sediments in the Dongping Lake, North China[J]. Quaternary International, 2023, 673: 53-61.

[104] Blatt H, Schultz D J. Size distribution of quartz in mudrocks[J]. Sedimentology, 1976, 23(6): 857-866.

[105] Milliken K L. Cathodoluminescent textures and the origin of quartz silt in Oligocene mudrocks, south Texas[J]. Journal of Sedimentary Research, 1994, 64(3a): 567-571.

[106] Chen D Z, Wang J G, Qing H R, et al. Hydrothermal venting activities in the Early Cambrian, South China: Petrological, geochronological and stable isotopic constraints[J]. Chemical Geology, 2009, 258(3/4): 168-181.

[107] Schieber J, Krinsley D, Riciputi L. Diagenetic origin of quartz silt in mudstones and implications for silica cycling[J]. Nature, 2000, 406(6799): 981-985.

[108] Zhao J H, Jin Z K, Jin Z J, et al. Origin of authigenic quartz in organic-rich shales of the Wufeng and Longmaxi Formations in the Sichuan Basin, South China: Implications for pore evolution[J]. Journal of Natural Gas Science and Engineering, 2017, 38: 21-38.

[109] Metwally Y M, Chesnokov E M. Clay mineral transformation as a major source for authigenic quartz in thermo-mature gas shale[J]. Applied Clay Science, 2012, 55: 138-150.

[110] Milliken K L, Ergene S M, Ozkan A. Quartz types, authigenic and detrital, in the Upper Cretaceous Eagle Ford Formation, South

Texas, USA[J]. Sedimentary Geology, 2016, 339: 273-288.

[111] Ye Y P, Tang S H, Xi Z D, et al. Quartz types in the Wufeng-Longmaxi Formations in southern China: Implications for porosity evolution and shale brittleness[J]. Marine and Petroleum Geology, 2022, 137: 105479.

[112] 冯冰，沈家宁，李龙，等. 黔北正安地区五峰组：龙马溪组页岩硅质矿物成因及意义[J]. 沉积与特提斯地质，2024，44（2）：399-410. [Feng Bing, Shen Jianing, Li Long, et al. Origins and significance of siliceous minerals in the shale reservoirs of the Wufeng-Longmaxi Formation in the Zheng'an area, northern Guizhou[J]. Sedimentary Geology and Tethyan Geology, 2024, 44(2): 399-410.]

[113] Thyberg B, Jahren J, Winje T, et al. Quartz cementation in Late Cretaceous mudstones, northern North Sea: Changes in rock properties due to dissolution of smectite and precipitation of micro-quartz crystals[J]. Marine and Petroleum Geology, 2010, 27(8): 1752-1764.

[114] 钟秋. 海相、海陆交互相页岩中石英成因及脆性指数对比研究[D]. 徐州：中国矿业大学，2021. [Zhong Qiu. Comparative study on the origin of quartz and brittleness index in marine and marine continental shale[D]. Xuzhou: China University of Mining and Technology, 2021.]

[115] Vos K, Vandenberghe N, Elsen J. Surface textural analysis of quartz grains by scanning electron microscopy (SEM): From sample preparation to environmental interpretation[J]. Earth-Science Reviews, 2014, 128: 93-104.

[116] 黄日辉，张立婷，冯淼彦，等. 广东省东海岛大岭剖面沉积物粒度、微形态特征与沉积环境[J]. 中国沙漠，2023，43（2）：121-129. [Huang Rihui, Zhang Liting, Feng Miaoyan, et al. Granularity, surface microtextural features and sedimentary environment of the Daling section in Donghai Island, Guangdong, China[J]. Journal of Desert Research, 2023, 43(2): 121-129.]

[117] 丁家翔，许欢，杜研，等. 风成砂岩的显微特征与鉴别方法：以山西宁武—静乐盆地天池河组为例[J/OL]. 沉积学报. https://doi.org/10.14027/j.issn.1000-0550.2023.042. [Ding Jiaxiang, Xu Huan, Du Yan, et al. Microscopic features and identification method of aeolian deposits: A case study from the Tianchihe Formation, Ningwu-Jingle Basin, Shanxi province[J/OL]. Acta Sedimentologica Sinica. https://doi.org/10.14027/j.issn.1000-0550.2023.042.]

[118] 田娅琪，周亚利，孙晓巍，等. 末次盛冰期以来浑善达克沙地光释光年代学及气候变化研究[J/OL]. 沉积学报. https://doi.org/10.14027/j.issn.1000-0550.2023.053. [Tian Yaqi, Zhou Yali, Sun Xiaowei, et al. Optically stimulated luminescence chronology and climate change in the otindag sandy land since the last glacial maximum[J/OL]. Acta Sedimentologica Sinica. https://doi.org/10.14027/j.issn.1000-0550.2023.053.]

[119] 魏月华. 滇西南澜沧群时代、属性和变质—热液历史研究：对原—古特提斯演化的制约[D]. 武汉：中国地质大学，2022. [Wei Yuehua. Constraining the age, nature and metamorphic-hydrothermal history of the Lancang Group, SW Yunnan, with implications to the Proto- and Paleo-Tethys evolution[D]. Wuhan: China University of Geosciences, 2022.]

[120] Zinkernagel U. Cathodoluminescence of quartz and its application to sandstone petrology[J]. Contributions to Sedimentary Geology, 1978, 4: 69.

[121] 王子腾. 鄂尔多斯盆地西缘羊虎沟组物源分析与沉积特征研究[D]. 成都：成都理工大学，2020. [Wang Ziteng. Provenance analysis and sedimentary characteristics of Yanghugou Formation in the western margin of the ordos Basin[D]. Chengdu: Chengdu University of Technology, 2020.]

[122] 袁圣强，窦立荣，程顶胜，等. 尼日尔 Termit 盆地油气成藏新认识与勘探方向[J]. 石油勘探与开发，2023，50（2）：238-249. [Yuan Shengqiang, Dou Lirong, Cheng Dingsheng, et al. New understanding and exploration direction of hydrocarbon accumulation in Termit Basin, Niger[J]. Petroleum Exploration and Development, 2023, 50(2): 238-249.]

[123] 张俊锋，肖永军，陈云锋，等. 柴北缘马海东地区路乐河组冲积扇特征[J]. 科学技术与工程，2022，22（31）：13680-13688. [Zhang Junfeng, Xiao Yongjun, Chen Yunfeng, et al. Alluvial fan characteristics of lulehe Formation in the mahaidong area of northern Qaidam Basin[J]. Science Technology and Engineering, 2022, 22(31): 13680-13688.]

[124] 赵建华，金之钧，金振奎，等. 四川盆地五峰组—龙马溪组含气页岩中石英成因研究[J]. 天然气地球科学，2016，27（2）：377-386. [Zhao Jianhua, Jin Zhijun, Jin Zhenkui, et al. The genesis of quartz in Wufeng-Longmaxi gas shales, Sichuan Basin[J]. Natural Gas Geoscience, 2016, 27(2): 377-386.]

[125] Peltonen C, Marcussen Ø, Bjørlykke K, et al. Clay mineral diagenesis and quartz cementation in mudstones: The effects of

smectite to illite reaction on rock properties[J]. Marine and Petroleum Geology, 2009, 26(6): 887-898.

[126] 刘洪林，彭平，周尚文，等. 四川盆地川东龙潭组页岩气地质特征及勘探方向探讨[C]//第 31 届全国天然气学术年会（2019）论文集（03 非常规气藏）. 合肥：中国石油学会天然气专业委员会，2019：15. [Liu Honglin, Peng Ping, Zhou Shangwen, et al. Discussion on the geological characteristics of shale gas and exploration directions in the Longtan Formation of eastern Sichuan Basin[C]//Proceedings of the 31st national natural gas academic annual conference (2019) (03 unconventional gas reservoirs). Hefei: Natural Gas Committee Of Chinese Petroleum Socie, 2019: 15.]

[127] 管全中. 四川盆地威远区块五峰—龙马溪组页岩储层精细刻画与甜点预测[D]. 北京：中国石油大学（北京），2020. [Guan Quanzhong. Fine characterization and sweet spot prediction of the Wufeng-Longmaxi Formations in Weiyuan area, Sichuan Basin[D]. Beijing: China University of Petroleum (Beijing), 2020.]

[128] 王濡岳，胡宗全，包汉勇，等. 四川盆地上奥陶统五峰组—下志留统龙马溪组页岩关键矿物成岩演化及其控储作用[J]. 石油实验地质，2021，43（6）：996-1005. [Wang Ruyue, Hu Zongquan, Bao Hanyong, et al. Diagenetic evolution of key minerals and its controls on reservoir quality of Upper Ordovician Wufeng-Lower Silurian Longmaxi shale of Sichuan Basin[J]. Petroleum Geology & Experiment, 2021, 43(6): 996-1005.]

[129] 李怡，石学文，罗超，等. 川南地区五峰组—龙马溪组页岩中成岩矿物的种类及其对储层的影响[J]. 成都理工大学学报（自然科学版），2024，51（5）：745-757，771. [Li Yi, Shi Xuewen, Luo Chao, et al. Impact of different diagenetic minerals on shale reservoirs in Wufeng-Longmaxi Formation in southern Sichuan Basin[J]. Journal of Chengdu University of Technology (Science & Technology Edition), 2024, 51(5): 745-757, 771.]

[130] 彭俊文. 氧化还原敏感元素在海相沉积物中富集的其他控制因素：海平面波动[J]. 中国科学（D 辑）：地球科学，2022，52(11)：2254-2274. [Peng Junwen. What besides redox conditions? Impact of sea-level fluctuations on redox-sensitive trace-element enrichment patterns in marine sediments[J]. Science China (Seri. D): Earth Sciences, 2022, 52(11): 2254-2274.]

[131] 王拔秀，张鹏辉，梁杰，等. 生物成因微晶石英特征及其对海相页岩储层孔隙发育的影响[J]. 沉积学报，2024，42（5）：1738-1752. [Wang Baxiu, Zhang Penghui, Liang Jie, et al. Biogenic microcrystalline quartz and its influence on pore development in marine shale reservoirs[J]. Acta Sedimentologica Sinica, 2024, 42(5): 1738-1752.]

[132] 卢龙飞，刘伟新，魏志红，等. 四川盆地志留系页岩成岩特征及其对孔隙发育与保存的控制[J]. 沉积学报，2022，40（1）：73-87. [Lu Longfei, Liu Weixin, Wei Zhihong, et al. Diagenesis of the Silurian Shale, Sichuan Basin: Focus on pore development and preservation[J]. Acta Sedimentologica Sinica, 2022, 40(1): 73-87.]

[133] 刘洪林，郭伟，刘德勋，等. 海相页岩成岩过程中的自生脆化作用[J]. 天然气工业，2018，38（5）：17-25. [Liu Honglin, Guo Wei, Liu Dexun, et al. Authigenic embrittlement of marine shale in the process of diagenesis[J]. Natural Gas Industry, 2018, 38(5): 17-25.]

[134] 罗凡，段轲，张号，等. 鄂西咸丰地区五峰组—龙马溪组火山凝灰岩发育特征及其对页岩有机质富集的影响[J]. 古地理学报，2024，26（5）：1058-1071. [Luo Fan, Duan Ke, Zhang Hao, et al. Development characteristics of volcanic tuff of the Wufeng-Longmaxi Formations in Xianfeng area of western Hubei and its influence on enrichment of organic matter in shale[J]. Journal of Palaeogeography (Chinese Edition), 2024, 26(5): 1058-1071.]

[135] 张建国，姜在兴，刘鹏，等. 陆相超细粒页岩油储层沉积机制与地质评价[J]. 石油学报，2022，43（2）：234-249. [Zhang Jianguo, Jiang Zaixing, Liu Peng, et al. Deposition mechanism and geological assessment of continental ultrafine-grained shale oil reservoirs[J]. Acta Petrolei Sinica, 2022, 43(2): 234-249.]

[136] 王俊怀，刘英辉，万策，等. 准噶尔盆地乌—夏地区二叠系风城组云质岩特征及成因[J]. 古地理学报，2014，16（2）：157-168. [Wang Junhuai, Liu Yinghui, Wan Ce, et al. Characteristics and origin of dolomitic tuff in the Permian Fengcheng Formation in Wu-Xia area of Junggar Basin[J]. Journal of Palaeogeography, 2014, 16(2): 157-168.]

[137] 何文军，吕正祥，彭妙，等. 准噶尔盆地玛湖凹陷二叠系风城组凝灰岩储层特征及成因分析[J]. 矿物岩石，2023，43（4）：109-119. [He Wenjun, Lü Zhengxiang, Peng Miao, et al. Characteristics and genetic analysis of Permian Fengcheng Formation tuff reservoir in Mahu Sag, Junggar Basin[J]. Mineralogy and Petrology, 2023, 43(4): 109-119.]

[138] 郝兵. 鄂尔多斯盆地志丹地区延长组低渗砂岩储层特征及影响因素[D]. 青岛：中国石油大学（华东），2021. [Hao Bing. Characteristics and controlling factors of low permeability sandstone reservoirs in the Yanchang Formation of the Zhidan area, Ordos

Basin[D]. Qingdao: China University of Petroleum (East China), 2021.]

[139] 刘国恒，黄志龙，郭小波，等. 新疆三塘湖盆地马朗凹陷中二叠统芦草沟组泥页岩层系 SiO_2 赋存状态与成因[J]. 地质学报，2016，90（6）：1220-1235. [Liu Guoheng, Huang Zhilong, Guo Xiaobo, et al. The SiO_2 occurrence and origin in the shale system of Middle Permian series Lucaogou Formation in Malang Sag, Santanghu Basin, Xinjiang[J]. Acta Geologica Sinica, 2016, 90(6): 1220-1235.]

[140] 高波，潘哲君，刘连杰，等. 松辽盆地徐家围子断陷沙河子组砂砾岩储层有效性综合评价[J/OL]. 吉林大学学报（地球科学版）. https://doi.org/10.13278/j.cnki.jjuese.20230115. [Gao Bo, Pan Zhejun, Liu Lianjie, et al. Shahezi Formation of Xujiaweizi fault Depression, Songliao Basin comprehensive evaluation on the effectiveness of conglomerate reservoir in[J/OL]. Journal of Jilin University (Earth Science Edition). https://doi.org/10.13278/j.cnki.jjuese.20230115.]

[141] Hower J, Eslinger E V, Hower M E, et al. Mechanism of burial metamorphism of argillaceous sediment: 1. Mineralogical and chemical evidence[J]. GSA Bulletin, 1976, 87(5): 725-737.

[142] 张永旺，蒋善斌，李峰. 东营凹陷沙河街组砂岩储层砂泥岩界面对长石溶蚀的影响[J]. 地质学报，2021，95（3）：883-894. [Zhang Yongwang, Jiang Shanbin, Li Feng. Influence of sandstone-shale contacts on feldspar diagenesis in the sandstone reservoir of the Shahejie Formation in the Dongying Depression, Bohai Bay Basin[J]. Acta Geologica Sinica, 2021, 95(3): 883-894.]

[143] 邱隆伟，姜在兴，操应长，等. 泌阳凹陷碱性成岩作用及其对储层的影响[J]. 中国科学（D 辑）：地球科学，2001，31（9）：752-759. [Qiu Longwei, Jiang Zaixing, Cao Yingchang, et al. Alkaline diagenesis and its influence on a reservoir in the Biyang Depression[J]. Science China (Seri. D): Earth Sciences, 2001, 31(9): 752-759.]

[144] 朱毅秀，金振奎，金科，等. 中国陆相湖盆细粒沉积岩岩石学特征及成岩演化表征：以四川盆地元坝地区下侏罗统大安寨段为例[J]. 石油与天然气地质，2021，42（2）：494-508. [Zhu Yixiu, Jin Zhenkui, Jin Ke, et al. Petrologic features and diagenetic evolution of fine-grained sedimentary rocks in continental lacustrine basins: A case study on the Lower Jurassic Da'anzhai member of Yuanba area, Sichuan Basin[J]. Oil & Gas Geology, 2021, 42(2): 494-508.]

[145] 万友利，丁晓琪，白晓亮，等. 塔中地区志留系海相碎屑岩储层石英溶蚀成因及影响因素分析[J]. 沉积学报，2014，32（1）：138-147. [Wan Youli, Ding Xiaoqi, Bai Xiaoliang, et al. Quartz dissolution causes and influencing factors in the Silurian marine clastic reservoir rocks in Central Tarim Basin[J]. Acta Sedimentologica Sinica, 2014, 32(1): 138-147.]

[146] 解馨慧，邓虎成，胡蓝霄，等. 湖相细粒沉积岩颗粒微观力学特征及类型划分：以鄂尔多斯盆地上三叠统延长组 7 段页岩为例[J]. 石油与天然气地质，2024，45（4）：1079-1088. [Xie Xinhui, Deng Hucheng, Hu Lanxiao, et al. Micromechanical characteristics and classification of the grains of lacustrine finegrained sedimentary rocks: A case study of shales in the 7th member of the Upper Triassic Yanchang Formation, Ordos Basin[J]. Oil & Gas Geology, 2024, 45(4): 1079-1088.]

[147] 冯家乐，杨升宇，胡钦红，等. 沧东凹陷孔二段页岩生排烃效率及对含油性的影响[J]. 中国石油大学学报（自然科学版），2024，48（2）：45-56. [Feng Jiale, Yang Shengyu, Hu Qinhong, et al. Hydrocarbon generation and expulsion efficiency and influence on oil bearing property of shale in the second member of Paleogene Kongdian Formation in Cangdong Sag[J]. Journal of China University of Petroleum (Edition of Natural Science), 2024, 48(2): 45-56.]

[148] 彭军，张新怡，许天宇，等. 四川盆地元坝地区千佛崖组二段细粒沉积岩岩相特征及储集性分析[J]. 石油实验地质，2024，46（2）：247-262. [Peng Jun, Zhang Xinyi, Xu Tianyu, et al. Lithofacies characteristics and reservoir capacity of fine-grained sedimentary rocks of second member of Qianfoya Formation in Yuanba area, Sichuan Basin[J]. Petroleum Geology & Experiment, 2024, 46(2): 247-262.]

[149] 于利民. 松辽盆地大情字井地区青山口组一段夹层型页岩油甜点综合评价[D]. 大庆：东北石油大学，2023. [Yu Limin. Comprehensive evaluation of sweet spots in interlayer shale oil of the first member of Qingshankou Formation in Daqingzijing area of the Songliao Basin[D]. Daqing: Northeast Petroleum University, 2023.]

[150] 秦恩鹏，张君莹，张生兵，等. 三塘湖盆地芦草沟组细粒岩储集层微观特征[J]. 新疆石油地质，2023，44（3）：299-306. [Qin Enpeng, Zhang Junying, Zhang Shengbing, et al. Microscopic characteristics of fine-grained reservoirs in Lucaogou Formation, Santanghu Basin[J]. Xinjiang Petroleum Geology, 2023, 44(3): 299-306.]

[151] Lerman A, Imboden D M, Gat J R, et al. Physics and chemistry of lakes[M]. Berlin: Springer-Verlag, 1995.

[152] Schieber J. Early diagenetic silica deposition in algal cysts and spores: A source of sand in black shales?[J]. Journal of Sedimentary

Research, 1996, 66(1): 175-183.

[153] Shi L, Squier T C, Zachara J M, et al. Respiration of metal (hydr)oxides by shewanella and geobacter: A key role for multihaem c-type cytochromes[J]. Molecular Microbiology, 2007, 65(1): 12-20.

[154] Konhauser K O, Urrutia M M. Bacterial clay authigenesis: A common biogeochemical process[J]. Chemical Geology, 1999, 161(4): 399-413.

[155] 李阳，李晓光，张廷山，等. 细粒岩天文旋回识别及在精细地层划分上的应用：以辽河西部凹陷雷家地区沙四段为例[J/OL]. 沉积学报. https://doi.org/10.14027/j.issn.1000-0550.2023.133. [LI Yang, LI Xiaoguang, ZHANG Tingshan, et al. Identification of astronomical cycles in fine-grained rocks and their application in fine stratigraphic division: A case study of the Fourth member of the Shahejie Formation in the Leijia area, western Sag of the Liaohe Depression[J/OL]. Acta Sedimentologica Sinica. https://doi.org/10.14027/j.issn.1000-0550.2023.133.]

[156] Xia R, Zhang J G, Zhong Q. Study on the differential distribution patterns of fine-grained sedimentary rocks in the Lower third member of the Shahejie Formation in Zhanhua Sag, Bohai Bay Basin[J]. Minerals, 2024, 14(1): 70.

[157] Sun N L, Chen T Y, Gao J B, et al. Lithofacies and reservoir characteristics of saline lacustrine fine-grained sedimentary rocks in the northern Dongpu Sag, Bohai Bay Basin: Implications for shale oil exploration[J]. Journal of Asian Earth Sciences, 2023, 252: 105686.

[158] 俞映月，吴世强，郑有恒，等. 江汉盆地陈沱口凹陷始新统盐湖古环境对富有机质岩相发育的控制[J]. 地质科技通报，2024，43（5）：70-80. [Yu Yingyue, Wu Shiqiang, Zheng Youheng, et al. Paleoenvironmental controls on organic-rich lithofacies of Eocene saline lacustrine in the Chentuokou Depression, Jianghan Basin[J]. Bulletin of Geological Science and Technology, 2024, 43(5): 70-80.]

[159] 周立宏，蒲秀刚，肖敦清，等. 渤海湾盆地沧东凹陷孔二段页岩油形成条件及富集主控因素[J]. 天然气地球科学，2018，29（9）：1323-1332. [Zhou Lihong, Pu Xiugang, Xiao Dunqing, et al. Geological conditions for shale oil Formation and the main controlling factors for the enrichment of the 2nd member of Kongdian Formation in the Cangdong Sag, Bohai Bay Basin[J]. Natural Gas Geoscience, 2018, 29(9): 1323-1332.]

[160] 邓远，陈世悦，蒲秀刚，等. 渤海湾盆地沧东凹陷孔店组二段细粒沉积岩形成机理与环境演化[J]. 石油与天然气地质，2020，41（4）：811-823，890. [Deng Yuan, Chen Shiyue, Pu Xiugang, et al. Formation mechanism and environmental evolution of fine-grained sedimentary rocks from the second member of Kongdian Formation in the Cangdong Sag, Bohai Bay Basin[J]. Oil & Natural Gas Geology, 2020, 41(4): 811-823, 890.]

[161] Zhao X Z, Zhou L H, Pu X G, et al. The sedimentary structure and petroleum geologic significance of the ring belt of the closed lake Basin: An integrated interpretation of well and seismic data of the Kong2 member in Cangdong Sag, Central Bohai Bay Basin, China[J]. Interpretation, 2018, 6(2): T283-T298.

[162] 肖贝，陈磊，杨骁，等. 准噶尔盆地深部咸水层 CO_2 地质封存适宜性及潜力评价[J]. 大庆石油地质与开发，2024，43（6）：120-127. [Xiao Bei, Chen Lei, Yang Huang, et al. Suitability and potential evaluation of CO_2 geological storage in deep saline aquifers of Junggar Basin[J]. Petroleum Geology & Oilfield Development in Daqing, 2024, 43(6): 120-127.]

[163] 潘永帅，黄志龙，郭小波，等. 火山灰影响下的湖相富有机质页岩油成藏条件分析：以三塘湖盆地条湖—马朗凹陷芦草沟组为例[J]. 地质学报，2022，96（3）：1053-1068. [Pan Yongshuai, Huang Zhilong, Guo Xiaobo, et al. Analysis of accumulation conditions of lacustrine organic-rich shale oil affected by volcanic ash: A case study of the Lucaogou Formation in the Tiaohu-Malang Sag, Santanghu Basin[J]. Acta Geologica Sinica, 2022, 96(3): 1053-1068.]

[164] 吴世强，陈凤玲，姜在兴，等. 江汉盆地潜江凹陷古近系潜江组白云岩成因[J]. 石油与天然气地质，2020，41（1）：201-208. [Wu Shiqiang, Chen Fengling, Jiang Zaixing, et al. Origin of Qianjiang Formation dolostone in Qianjiang Sag, Jianghan Basin[J]. Oil & Gas Geology, 2020, 41(1): 201-208.]

[165] 徐崇凯，刘池洋，郭佩，等. 潜江凹陷古近系潜江组盐间泥岩地球化学特征及地质意义[J]. 沉积学报，2018，36（3）：617-629. [Xu Chongkai, Liu Chiyang, Guo Pei, et al. Geochemical characteristics and their geological significance of intrasalt mudstones from the Paleogene Qianjiang Formation in the Qianjiang Graben, Jianghan Basin, China[J]. Acta Sedimentologica Sinica, 2018, 36(3): 617-629.]

[166] 张永生，王国力，杨玉卿，等. 江汉盆地潜江凹陷古近系盐湖沉积盐韵律及其古气候意义[J]. 古地理学报，2005，7（4）：461-470. [Zhang Yongsheng, Wang Guoli, Yang Yuqing, et al. Rhythms of saline lake sediments of the Paleogene and their paleoclimatic significance in Qianjiang Sag, Jianghan Basin[J]. Journal of Palaeogeography, 2005, 7(4): 461-470.]

[167] 陈森然，刘诗琦，刘新社，等. 碳酸盐岩成岩重结晶作用及其储层意义[J]. 北京大学学报（自然科学版），2024，60（5）：839-850. [Chen Senran, Liu Shiqi, Liu Xinshe, et al. Diagenetic recrystallization of carbonate and its significance for reservoir[J]. Acta Scientiarum Naturalium Universitatis Pekinensis, 2024, 60(5): 839-850.]

[168] 韩豫，操应长，梁超，等. 川南地区五峰组—龙马溪组沉积环境演化及其对页岩发育的控制[J]. 中国石油大学学报（自然科学版），2024，48（2）：11-23. [Han Yu, Cao Yingchang, Liang Chao, et al. Sedimentary environment evolution of Wufeng Formation-Longmaxi Formation and its control on shale deposition in the southern Sichuan Basin[J]. Journal of China University of Petroleum (Edition of Natural Science), 2024, 48(2): 11-23.]

[169] 张欢，曾翔，刘惠民，等. 泥页岩纹层矿物—有机质特征与成因差异及其对页岩油生储意义：以渤海湾盆地东营凹陷沙三下亚段—沙四上亚段为例[J]. 天然气地球科学，2024，35（7）：1261-1276. [Zhang Huan, Zeng Xiang, Liu Huimin, et al. The characteristics and genetic differences of mineral organic matter in shale laminae and its significance to shale oil generation and storage: A case study of the Lower submember of the third member and Upper submember of the fourth member in Shahejie Formation in Dongying Sag, Bohai bay Basin[J]. Natural Gas Geoscience, 2024, 35(7): 1261-1276.]

[170] 滕建彬. 东营凹陷利页 1 井泥页岩中白云石成因及层序界面意义[J]. 油气地质与采收率，2018，25（2）：1-7，36. [Teng Jianbin. Genesis of dolomite in shale drilled by Well Liye1 in Dongying Sag and its significance on sequence boundary indication[J]. Petroleum Geology and Recovery Efficiency, 2018, 25(2): 1-7, 36.]

[171] 朱光有，李茜. 白云岩成因类型与研究方法进展[J]. 石油学报，2023，44（7）：1167-1190. [Zhu Guangyou, Li Xi. Progress in genetic types and research methods of dolomite[J]. Acta Petrolei Sinica, 2023, 44(7): 1167-1190.]

[172] 李茜，朱光有，张志遥. 超深层白云岩成因与规模储层控制因素：以四川盆地震旦系灯影组和寒武系龙王庙组为例[J]. 中国科学（D 辑）：地球科学，2024，54（7）：2389-2418. [Li Xi, Zhu Guangyou, Zhang Zhiyao. Genesis of ultra-deep dolostone and controlling factors of large-scale reservoir: A case study of the Sinian Dengying Formation and the Cambrian Longwangmiao Formation in the Sichuan Basin[J]. Science China (Seri. D): Earth Sciences, 2024, 54(7): 2389-2418.]

[173] Stabel H H. Calcite precipitation in Lake Constance: Chemical equilibrium, sedimentation, and nucleation by algae[J]. Limnology and Oceanography, 1986, 31(5): 1081-1094.

[174] Macquaker J H S, Bentley S J, Bohacs K M. Wave-enhanced sediment-gravity flows and mud dispersal across continental shelves: Reappraising sediment transport processes operating in ancient mudstone successions[J]. Geology, 2010, 38(10): 947-950.

[175] Dupraz C, Reid R P, Braissant O, et al. Processes of carbonate precipitation in modern microbial mats[J]. Earth-Science Reviews, 2009, 96(3): 141-162.

[176] Bluszcz P, Lücke A, Ohlendorf C, et al. Seasonal dynamics of stable isotopes and element ratios in authigenic calcites during their precipitation and dissolution, Sacrower See (northeastern Germany)[J]. Journal of Limnology, 2009, 68(2): 257-273.

[177] Kelts K, Hsü K J. Freshwater carbonate sedimentation[M]//Lerman A. Lakes. New York: Springer, 1978: 295-323.

[178] 王铭乾，张元元，朱如凯，等. 湖泊细粒沉积岩纹层特征与形成机制研究进展及展望[J/OL]. 沉积学报. https://doi.org/10.14027/j.issn.1000-0550.2024.080. [Wang Mingqian, Zhang Yuanyuan, Zhu Rukai, et al. Progress and perspective on the characteristics and Formation mechanism of laminae in lacustrine fine-grained sedimentary rocks[J/OL]. Acta Sedimentologica Sinica. https://doi.org/10.14027/j.issn.1000-0550.2024.080.]

[179] Ma J, Wu C D, Wang Y Z, et al. Paleoenvironmental reconstruction of a saline lake in the Tertiary: Evidence from aragonite laminae in the northern Tibet Plateau[J]. Sedimentary Geology, 2017, 353: 1-12.

[180] Krause S, Liebetrau V, Gorb S, et al. Microbial nucleation of Mg-rich dolomite in exopolymeric substances under anoxic modern seawater salinity: New insight into an old enigma[J]. Geology, 2012, 40(7): 587-590.

[181] Suosaari E P, Lascu I, Oehlert A M, et al. Authigenic clays as precursors to carbonate precipitation in saline lakes of Salar de Llamara, northern Chile[J]. Communications Earth & Environment, 2022, 3(1): 325.

[182] De Muynck W, De Belie N, Verstraete W. Microbial carbonate precipitation in construction materials: A review[J]. Ecological

Engineering, 2010, 36(2): 118-136.

[183] Pacton M, Fiet N, Gorin G E. Bacterial activity and preservation of sedimentary organic matter: The role of exopolymeric substances[J]. Geomicrobiology Journal, 2007, 24(7/8): 571-581.

[184] Decho A W, Gutierrez T. Microbial extracellular polymeric substances (EPSs) in ocean systems[J]. Frontiers in Microbiology, 2017, 8: 922.

[185] 冯骁，邓泽，郭红光，等. 地质封存二氧化碳微生物转化研究进展[J]. 生物工程学报，2024，40（9）：2884-2898. [Feng Xiao, Deng Ze, Guo Hongguang, et al. Research advances of microbial transformation of CO_2 in geological sequestration[J]. Chinese Journal of Biotechnology, 2024, 40(9): 2884-2898.]

[186] 韩舒筠，于炳松，白辰阳，等. 渤海湾盆地东营凹陷沙河街组泥晶碳酸盐岩中的微生物沉积作用[J]. 矿物岩石，2018，38（2）：104-113. [Han Shuyin, Yu Bingsong, Bai Chenyang, et al. Microbial sedimentation of shahejie Formation micritic carbonate in the Dongying Depression, Bohai bay Basin[J]. Journal of Mineralogy and Petrology, 2018, 38(2): 104-113.]

[187] 王金艺，金振奎. 微生物白云岩形成机理、识别标志及存在的问题[J]. 沉积学报，2022，40（2）：350-359. [Wang Jinyi, Jin Zhenkui. Formation mechanism, identification markers, and questions regarding microbial dolomite[J]. Acta Sedimentologica Sinica, 2022, 40(2): 350-359.]

[188] 滕建彬，邱隆伟，张守鹏，等. 济阳坳陷古近系沙河街组湖相富有机质页岩白云石成因及成岩演化[J]. 石油勘探与开发，2022，49（6）：1080-1093. [Teng Jianbin, Qiu Longwei, Zhang Shoupeng, et al. Origin and diagenetic evolution of dolomites in Paleogene Shahejie Formation lacustrine organic shale of Jiyang Depression, Bohai Bay Basin, East China[J]. Petroleum Exploration and Development, 2022, 49(6): 1080-1093.]

[189] Guo P, Wen H G, Li C Z, et al. Lacustrine dolomite in deep time: What really matters in early dolomite Formation and accumulation?[J]. Earth-Science Reviews, 2023, 246: 104575.

[190] Becker A, Bismayer U, Epple M, et al. Structural characterisation of X-ray amorphous calcium carbonate (ACC) in sternal deposits of the Crustacea *Porcellio scaber*[J]. Dalton Transactions, 2003(4): 551-555.

[191] 崔航，朱世发，施振生，等. 川北侏罗系大安寨段湖相混积层系沉积特征与发育模式[J]. 古地理学报，2022，24（6）：1099-1113. [Cui Hang, Zhu Shifa, Shi Zhensheng, et al. Sedimentary characteristics and development model of lacustrine fine-grained hybrid sedimentary rocks in the Jurassic Da'anzhai member, northern Sichuan Basin[J]. Journal of Palaeogeography (Chinese Edition), 2022, 24(6): 1099-1113.]

[192] 李倩文，刘忠宝，陈斐然，等. 四川盆地侏罗系页岩层系岩相类型及储集特征：以元坝地区 Y2 井大安寨段为例[J]. 石油与天然气地质，2022，43（5）：1127-1140. [Li Qianwen, Liu Zhongbao, Chen Feiran, et al. Lithofacies types and reservoir characteristics of Jurassic shale in the Sichuan Basin revealed by the Da'anzhai member, Well Y2, Yuanba area[J]. Oil & Gas Geology, 2022, 43(5): 1127-1140.]

[193] Anjos S M C, Passarelli F M, Wambersie O E, et al. Libra: Applied technologies adding value to a giant ultra deep water pre-salt field - Santos Basin, Brazil[C]//Proceedings of the offshore technology conference Brasil. Rio de Janeiro: OTC, 2019.

[194] Watabe K, Kaesler R L. Ontogeny of a new species of paraparchites (ostracoda) from the Lower Permian speiser shale in Kansas[J]. Journal of Paleontology, 2004, 78(3): 603-611.

[195] 辛利伟，李虎，王晓蕾，等. 四川盆地龙马溪组与大安寨段页岩储层特征对比研究：海相与湖相的差异分析[J]. 地质科学，2024，59（4）：1003-1017. [Xin Liwei, Li Hu, Wang Xiaolei, et al. Comparative study of shale reservoir characteristics between the Longmaxi Formation and the Da'anzhai member in the Sichuan Basin: Highlighting facies differences between marine and lacustrine depositional environments[J]. Chinese Journal of Geology, 2024, 59(4): 1003-1017.]

[196] 蒋代琴，李平平，邹华耀. 川东北元坝地区侏罗系陆相页岩天然裂缝发育特征及其对页岩油气富集和保存的影响[J]. 现代地质，2024，38（2）：362-372. [Jiang Daiqin, Li Pingping, Zou Huayao. Characteristics of natural fractures and their influence on oil and gas enrichment and preservation of the Jurassic continental shale in the Yuanba area, Northeastern Sichuan Basin[J]. Geoscience, 2024, 38(2): 362-372.]

[197] 刘树根，邓宾，孙玮，等. 四川盆地是“超级”的含油气盆地吗?[J]. 西华大学学报（自然科学版），2020，39（5）：20-35. [Liu Shugen, Deng Bin, Sun Wei, et al. May Sichuan Basin be a super petroliferous Basin?[J]. Journal of Xihua University (Natural

Science Edition), 2020, 39(5): 20-35.]

[198] 王鑫，蒙启安，白云风，等. 页岩储集性与含油性的毫米级精细评价及意义：以松辽盆地青山口组一段为例[J]. 石油学报，2024，45（6）：961-975. [Wang Xin, Meng Qi'an, Bai Yunfeng, et al. Millimeter-scale fine evaluation and significance of shale reservoir performance and oil-bearing property: A case study of member 1 of Qingshankou Formation in Songliao Basin[J]. Acta Petrolei Sinica, 2024, 45(6): 961-975.]

[199] 王成善，冯志强，吴河勇，等. 中国白垩纪大陆科学钻探工程：松科一井科学钻探工程的实施与初步进展[J]. 地质学报，2008，82（1）：9-20. [Wang Chengshan, Feng Zhiqiang, Wu Heyong, et al. Preliminary achievement of the Chinese Cretaceous continental scientific drilling project-SK-I[J]. Acta Geologica Sinica, 2008, 82(1): 9-20.]

[200] 刘中戎，陈孔全，范志伟，等. 羌塘盆地西北部中侏罗统布曲组地层沉积特征[J/OL]. 沉积与特提斯地质. https://doi.org/10.19826/j.cnki.1009-3850.2024.04003. [Liu Zhongrong, Chen Kongquan, Fan Zhiwei, et al. Lithofacies paleogeographic characteristics of the Middle Jurassic Buqu Formation in the northwest Qiangtang Basin[J/OL]. Sedimentary Geology and Tethyan Geology. https://doi.org/10.19826/j.cnki.1009-3850.2024.04003.]

[201] 胡素云，陶士振，闫伟鹏，等. 中国陆相致密油富集规律及勘探开发关键技术研究进展[J]. 天然气地球科学，2019，30（8）：1083-1093. [Hu Suyun, Tao Shizhen, Yan Weipeng, et al. Advances on continental tight oil accumulation and key technologies for exploration and development in China[J]. Natural Gas Geoscience, 2019, 30(8): 1083-1093.]

[202] 王永炜，李荣西，高胜利，等. 渤海湾盆地黄骅坳陷湖相碳酸盐岩微量元素特征及沉积环境[J]. 石油实验地质，2017，39（6）：849-857. [Wang Yongwei, Li Rongxi, Gao Shengli, et al. Trace element characteristics and sedimentary environment of lacustrine carbonate rocks in the Huanghua Depression, Bohai Bay Basin[J]. Petroleum Geology & Experiment, 2017, 39(6): 849-857.]

[203] 彭军，杨一茗，刘惠民，等. 陆相湖盆细粒混积岩的沉积特征与成因机理：以东营凹陷南坡陈官庄地区沙河街组四段上亚段为例[J]. 石油学报，2022，43（10）：1409-1426. [Peng Jun, Yang Yiming, Liu Huimin, et al. Sedimentary characteristics and genetic mechanism of fine-grained hybrid sedimentary rocks in continental lacustrine Basin: A case study of the Upper submember of member 4 of Shahejie Formation in Chenguanzhuang area, southern slope of Dongying Sag[J]. Acta Petrolei Sinica, 2022, 43(10): 1409-1426.]

[204] Landmann G, Reimer A, Kempe S. Climatically induced lake level changes at Lake Van, Turkey, during the Pleistocene/Holocene transition[J]. Global Biogeochemical Cycles, 1996, 10(4): 797-808.

[205] 张奎华，张鹏飞，苗卓伟，等. 地球轨道参数振幅与深水环境白云石化强度波动[J/OL]. 古地理学报. http://kns.cnki.net/kcms/detail/11.4678.P.20240611.1611.004.html. [Zhang Kuihua, Zhang Pengfei, Miao Zhuowei, et al. Amplitude of earth's orbital parameters and fluctuations of deep-water dolomitization[J/OL]. Journal of Palaeogeography (Chinese Edition). http://kns.cnki.net/kcms/detail/11.4678.P.20240611.1611.004.html.]

[206] 魏世林，焦鑫，柳益群，等. 陆内裂谷湖相火山—热液沉积型白云岩研究进展[J]. 古地理学报，2024，26（5）：1037-1057. [Wei Shilin, Jiao Xin, Liu Yiqun, et al. Progress on volcanic-hydrothermal sedimentary dolostone in intracontinental lacustrine rift Basin[J]. Journal of Palaeogeography (Chinese Edition), 2024, 26(5): 1037-1057.]

[207] 肖杰. 玛湖凹陷二叠系风城组碱湖形成机理及其演化[D]. 青岛：中国石油大学（华东），2020. [Xiao Jie. Formation mechanism and evolution of the alkaline Lakes of the Permian Fengcheng Formation in the Mahu Depression[D]. Qingdao: China University of Petroleum (East China), 2020.]

[208] 柳益群，周鼎武，南云，等. 新疆北部地区二叠系幔源碳酸岩质喷积岩研究[J]. 古地理学报，2018，20（1）：49-63. [Liu Yiqun, Zhou Dingwu, Nan Yun, et al. Permian mantle-derived carbonatite originated exhalative sedimentary rocks in North Xinjiang[J]. Journal of Palaeogeography (Chinese Edition), 2018, 20(1): 49-63.]

[209] Wilkin R T, Barnes H L, Brantley S L. The size distribution of framboidal pyrite in modern sediments: An indicator of redox conditions[J]. Geochimica et Cosmochimica Acta, 1996, 60(20): 3897-3912.

[210] Wignall P B, Bond D P G, Kuwahara K, et al. An 80 million year oceanic redox history from Permian to Jurassic pelagic sediments of the Mino-Tamba terrane, SW Japan, and the origin of four mass extinctions[J]. Global and Planetary Change, 2010, 71(1/2): 109-123.

[211] Gomes M L, Klatt J M, Dick G J, et al. Sedimentary pyrite sulfur isotope compositions preserve signatures of the surface microbial mat environment in sediments underlying low-oxygen cyanobacterial mats[J]. Geobiology, 2022, 20(1): 60-78.

[212] 邓乃尔，徐浩，周文，等. 基于深度学习的页岩黄铁矿扫描电镜图像分割及环境指示意义：以四川盆地泸州Ⅰ区为例[J]. 地球科学进展，2024，39（5）：476-488. [Deng Naier, Xu Hao, Zhou Wen, et al. Deep learning SEM image segmentation of shale pyrite and environmental indications: A study of Luzhou Block, Sichuan Basin[J]. Advances in Earth Science, 2024, 39(5): 476-488.]

[213] 何贤科，李文俊，段冬平，等. 西湖凹陷平湖斜坡北段平湖组薄煤层与泥岩的微观岩石学特征及其沉积学意义[J]. 海洋地质与第四纪地质，2024，44（2）：210-222. [He Xianke, Li Wenjun, Duan Dongping, et al. Micro-petrological characteristics and its sedimentological significance of thin coal seam and mudstone in Pinghu Formation in the northern part of Pinghu Slope, Xihu Sag[J]. Marine Geology & Quaternary Geology, 2024, 44(2): 210-222.]

[214] 刘江艳，李士祥，李桢，等. 鄂尔多斯盆地长7_3亚段泥页岩黄铁矿发育特征及其地质意义[J]. 天然气地球科学，2021，32（12）：1830-1838. [Liu Jiangyan, Li Shixiang, Li Zhen, et al. Characteristics and geological significance of pyrite in Chang 7_3 sub-member in the Ordos Basin[J]. Natural Gas Geoscience, 2021, 32(12): 1830-1838.]

[215] Tribovillard N, Bout-Roumazeilles V, Delattre M, et al. Sedimentary pyrite as a trap of organic matter: Preliminary results from large-framboid observation[J]. European Journal of Mineralogy, 2022, 34(1): 77-83.

[216] Ohfuji H, Rickard D. Experimental syntheses of framboids: A review[J]. Earth-Science Reviews, 2005, 71(3/4): 147-170.

[217] 刘治成，赵伟，文俊，等. 川南上二叠统宣威组底部黏土岩型镓矿地球化学特征及镓元素的富集成因[J]. 矿物岩石，2024，44（2）：74-87. [Liu Zhicheng, Zhao Wei, Wen Jun, et al. Geochemical characteristics of claystone type gallium deposits at the bottom of the Upper Permian Xuanwei Formation in southern Sichuan and origin of gallium enrichment[J]. Mineralogy and Petrology, 2024, 44(2): 74-87.]

[218] Raiswell R, Canfield D E. The iron biogeochemical cycle past and present[J]. Geochemical Perspectives, 2012, 1(1): 1-220.

[219] Liang C, Ji S C, Cao Y C, et al. Characteristics, origins, and significance of pyrites in deep-water shales[J]. Science China Earth Sciences, 2024, 67(2): 313-342.

[220] Norman L, Cabanesa D J E, Blanco-Ameijeiras S, et al. Iron biogeochemistry in aquatic systems: From source to bioavailability[J]. Chimia, 2014, 68(11): 764-771.

[221] Tagliabue A, Bowie A R, Boyd P W, et al. The integral role of iron in ocean biogeochemistry[J]. Nature, 2017, 543(7643): 51-59.

[222] Lovley D R. Microbial Fe(III) reduction in subsurface environments[J]. FEMS Microbiology Reviews, 1997, 20(3/4): 305-313.

[223] Wang C L, Zhai M G, Robbins L J, et al. Late Archean shelf-to-Basin iron shuttle contributes to the Formation of the world-class Dataigou banded iron Formation[J]. Economic Geology, 2024, 119(3): 725-736.

[224] Mänd K, Lalonde S V, Paiste K, et al. Iron isotopes reveal a benthic iron shuttle in the Palaeoproterozoic Zaonega Formation: Basinal restriction, euxinia, and the effect on global palaeoredox proxies[J]. Minerals, 2021, 11(4): 368.

[225] Rickard D. Framboids[M]. Oxford: Oxford University Press, 2021.

[226] Machel H G. Bacterial and thermochemical sulfate reduction in diagenetic settings: Old and new insights[J]. Sedimentary Geology, 2001, 140(1/2): 143-175.

[227] Cai C F, Li H X, Li K K, et al. Thermochemical sulfate reduction in sedimentary basins and beyond: A review[J]. Chemical Geology, 2022, 607: 121018.

[228] Ryu J H, Zierenberg R A, Dahlgren R A, et al. Sulfur biogeochemistry and isotopic fractionation in shallow groundwater and sediments of Owens Dry Lake, California[J]. Chemical Geology, 2006, 229(4): 257-272.

[229] Nara F W, Watanabe T, Kakegawa T, et al. Climate control of sulfate influx to Lake Hovsgol, northwest Mongolia, during the last glacial–postglacial transition: Constraints from sulfur geochemistry[J]. Palaeogeography, Palaeoclimatology, Palaeoecology, 2010, 298(3/4): 278-285.

[230] Jørgensen B B, Isaksen M F, Jannasch H W. Bacterial sulfate reduction above 100° C in deep-sea hydrothermal vent sediments[J]. Science, 1992, 258(5089): 1756-1757.

[231] Rickard D. Sedimentary pyrite framboid size-frequency distributions: A meta-analysis[J]. Palaeogeography, Palaeoclimatology, Palaeoecology, 2019, 522: 62-75.

[232] Lin Q, Wang J S, Algeo T J, et al. Enhanced framboidal pyrite Formation related to anaerobic oxidation of methane in the sulfate-methane transition zone of the northern South China Sea[J]. Marine Geology, 2016, 379: 100-108.

[233] Liu J R, Pellerin A, Wang J S, et al. Multiple sulfur isotopes discriminate organoclastic and methane-based sulfate reduction by sub-seafloor pyrite Formation[J]. Geochimica et Cosmochimica Acta, 2022, 316: 309-330.

[234] Treude T, Niggemann J, Kallmeyer J, et al. Anaerobic oxidation of methane and sulfate reduction along the Chilean continental margin[J]. Geochimica et Cosmochimica Acta, 2005, 69(11): 2767-2779.

[235] Reeburgh W S. Oceanic methane biogeochemistry[J]. Chemical Reviews, 2007, 107(2): 486-513.

[236] Wang M, Cai F, Li Q, et al. Characteristics of authigenic pyrite and its sulfur isotopes influenced by methane seep at Core A, Site 79 of the Middle Okinawa Trough[J]. Science China Earth Sciences, 2015, 58(12): 2145-2153.

[237] Lin Z Y, Sun X M, Lu Y, et al. The enrichment of heavy iron isotopes in authigenic pyrite as a possible indicator of sulfate-driven anaerobic oxidation of methane: Insights from the South China Sea[J]. Chemical Geology, 2017, 449: 15-29.

[238] 陈杨，金鑫，郎咸国，等. 鄂尔多斯盆地 T-OAE 时期湖泊硫循环及其地质意义[J/OL]. 沉积学报. https://doi.org/10.14027/j.issn.1000-0550.2023.112. [Chen Yang, Jin Xin, Lang Xianguo, et al. Sulfur cycle change and its geological significance during the Toarcian oceanic anoxic event (T-OAE) in the Ordos Basin[J/OL]. Acta Sedimentologica Sinica. https://doi.org/10.14027/j.issn.1000-0550.2023.112.]

[239] Miao X M, Feng X L, Liu X T, et al. Effects of methane seepage activity on the morphology and geochemistry of authigenic pyrite[J]. Marine and Petroleum Geology, 2021, 133: 105231.

[240] Ohmoto H. Stable isotope geochemistry of ore deposits[J]. Reviews in Mineralogy and Geochemistry, 1986, 16(1): 491-559.

[241] Machel H G, Krouse H R, Sassen R. Products and distinguishing criteria of bacterial and thermochemical sulfate reduction[J]. Applied Geochemistry, 1995, 10(4): 373-389.

[242] Cai C F, Zhang C M, Cai L L, et al. Origins of Palaeozoic oils in the Tarim Basin: Evidence from sulfur isotopes and biomarkers[J]. Chemical Geology, 2009, 268(3/4): 197-210.

[243] Cai C F, Zhang C M, Worden R H, et al. Application of sulfur and carbon isotopes to oil-source rock correlation: A case study from the Tazhong area, Tarim Basin, China[J]. Organic Geochemistry, 2015, 83-84: 140-152.

[244] Cai C F, Hu W S, Worden R H. Thermochemical sulphate reduction in Cambro-Ordovician carbonates in Central Tarim[J]. Marine and Petroleum Geology, 2001, 18(6): 729-741.

[245] Orr W L. Changes in sulfur content and isotopic ratios of sulfur during petroleum maturation: Study of Big Horn Basin Paleozoic oils[J]. AAPG Bulletin, 1974, 58(11): 2295-2318.

[246] Cui H, Kitajima K, Spicuzza M J, et al. Questioning the biogenicity of Neoproterozoic superheavy pyrite by SIMS[J]. American Mineralogist, 2018, 103(9): 1362-1400.

[247] Tyson R. The biomarker guide. Volume 1: Biomarkers and isotopes in the environment and human history. volume 2: Biomarkers and isotopes in petroleum exploration and earth history[J]. Geological Magazine, 2006, 143(2): 249-250.

[248] Walters C C, Wang F C, Qian K N, et al. Petroleum alteration by thermochemical sulfate reduction: A comprehensive molecular study of aromatic hydrocarbons and polar compounds[J]. Geochimica et Cosmochimica Acta, 2015, 153: 37-71.

[249] 罗厚勇，刘文汇，腾格尔，等. 碳酸盐岩储层原油裂解过程中的钙、硫分子地球化学研究：同步辐射 XANES 技术的应用[J]. 地质学报，2017，91（3）：668-677. [Luo Houyong, Liu Wenhui, Tenge, et al. Molecular geochemistry study of calcium and sulfur in the process of crude oil cracking in carbonatic rock reservoirs: Application of synchrotron radiation XANES technology[J]. Acta Geologica Sinica, 2017, 91(3): 668-677.]

[250] Amrani A, Zhang T W, Ma Q S, et al. The role of labile sulfur compounds in thermochemical sulfate reduction[J]. Geochimica et Cosmochimica Acta, 2008, 72(12): 2960-2972.

[251] Ma Q S, Ellis G S, Amrani A, et al. Theoretical study on the reactivity of sulfate species with hydrocarbons[J]. Geochimica et Cosmochimica Acta, 2008, 72(18): 4565-4576.

[252] Liu B, Mastalerz M, Schieber J. SEM petrography of dispersed organic matter in black shales: A review[J]. Earth-Science Reviews, 2022, 224: 103874.

[253] Cardott B J, Landis C R, Curtis M E. Post-oil solid bitumen network in the Woodford Shale, USA: A potential primary migration pathway[J]. International Journal of Coal Geology, 2015, 139: 106-113.

[254] 刘忠，唐书恒，张鹏豹，等. 煤系页岩有机质特征及有机碳含量预测：以宁武南区块为例[J]. 科学技术与工程，2023，23（27）：11593-11604. [Liu Zhong, Tang Shuheng, Zhang Pengbao, et al. Organic matter characteristics and total organic carbon content prediction of coal measure shale: A case study of the South Ningwu block[J]. Science Technology and Engineering, 2023, 23(27): 11593-11604.]

[255] 焦淑静，张慧，薛东川. 三塘湖盆地芦草沟组页岩有机显微组分扫描电镜研究[J]. 电子显微学报，2019，38（3）：257-263. [Jiao Shujing, Zhang Hui, Xue Dongchuan. SEM study on organic macerals of shale in Lucaogou Formation Santanghu Basin[J]. Journal of Chinese Electron Microscopy Society, 2019, 38(3): 257-263.]

[256] 刘贝. 泥页岩中有机质：类型、热演化与有机孔隙[J]. 地球科学，2023，48（12）：4641-4657. [Liu Bei. Organic matter in shales: Types, thermal evolution, and organic pores[J]. Earth Science, 2023, 48(12): 4641-4657.]

[257] 何燚. 川东—黔北地区龙潭组海陆过渡相页岩岩相与有机质特征[D]. 北京：中国地质大学（北京），2021. [He Yi. Lithofacies and Characteristics of organic matter in transitional facies shale of the Longtan Formation in eastern Sichuan and northern Guizhou[D]. Beijing: China University of Geosciences (Beijing), 2021.]

[258] 贾云倩，刘子平，任晓海，等. 有机质类型分异规律及其主控机制：以威远志留系龙马溪组页岩储层为例[J]. 沉积学报，2021，39（2）：341-352. [Jia Yunqian, Liu Ziping, Ren Xiaohai, et al. Organic matter type differentiation process and main control mechanism: Case study of the Silurian Longmaxi Formation shale reservoir in Weiyuan area[J]. Acta Sedimentologica Sinica, 2021, 39(2): 341-352.]

[259] 焦淑静，张慧，薛东川，等. 泥页岩有机显微组分的扫描电镜形貌特征及识别方法[J]. 电子显微学报，2018，37（2）：137-144. [Jiao Shujing, Zhang Hui, Xue Dongchuan, et al. Morphological structure and identify method of organic macerals of shale with SEM[J]. Journal of Chinese Electron Microscopy Society, 2018, 37(2): 137-144.]

[260] Stopes M C. On the petrology of banded bituminous coals[J]. Colliery Guardian, 1935,150(3684): 111-113.

[261] Pickel W, Kus J, Flores D, et al. Classification of liptinite - ICCP System 1994[J]. International Journal of Coal Geology, 2017, 169: 40-61.

[262] 刘思逸，高平，肖贤明，等. 四川盆地五峰—龙马溪组黑色页岩有机岩石学特征研究[J]. 现代地质，2022，36（5）：1281-1291. [Liu Siyi, Gao Ping, Xiao Xianming, et al. Study on organic petrology characteristics of the Wufeng-Longmaxi Formation black shale, Sichuan Basin[J]. Geoscience, 2022, 36(5): 1281-1291.]

[263] 谢国梁，刘树根，焦堃，等. 受显微组分控制的深层页岩有机质孔隙：四川盆地五峰组—龙马溪组有机质组分分类及其孔隙结构特征[J]. 天然气工业，2021，41（9）：23-34. [Xie Guoliang, Liu Shugen, Jiao Kun, et al. Organic pores in deep shale controlled by macerals: Classification and pore characteristics of organic matter components in Wufeng Formation-Longmaxi Formation of the Sichuan Basin[J]. Natural Gas Industry, 2021, 41(9): 23-34.]

[264] Kus J, Araujo C V, Borrego A G, et al. Identification of alginite and bituminite in rocks other than coal. 2006, 2009, and 2011 round robin exercises of the ICCP Identification of Dispersed Organic Matter Working Group[J]. International Journal of Coal Geology, 2017, 178: 26-38.

[265] Teng J, Mastalerz M, Liu B. Petrographic and chemical structure characteristics of amorphous organic matter in marine black shales: Insights from Pennsylvanian and Devonian black shales in the Illinois Basin[J]. International Journal of Coal Geology, 2021, 235: 103676.

[266] Reyes J, Jiang C, Lavoie D, et al. Organic petrographic analysis of artificially matured chitinozoan- and graptolite-rich Upper Ordovician shale from Hudson Bay Basin, Canada[J]. International Journal of Coal Geology, 2018, 199: 138-151.

[267] Petersen H I, Schovsbo N H, Nielsen A T. Reflectance measurements of zooclasts and solid bitumen in Lower Paleozoic shales, southern Scandinavia: Correlation to vitrinite reflectance[J]. International Journal of Coal Geology, 2013, 114: 1-18.

[268] Luo Q Y, Zhang L, Zhong N N, et al. Thermal evolution behavior of the organic matter and a ray of light on the origin of vitrinite-like maceral in the Mesoproterozoic and Lower Cambrian black shales: Insights from artificial maturation[J]. International Journal of Coal Geology, 2021, 244: 103813.

[269] Gao P, Liu G D, Lash G G, et al. Occurrences and origin of reservoir solid bitumen in Sinian Dengying Formation dolomites of the Sichuan Basin, SW China[J]. International Journal of Coal Geology, 2018, 200: 135-152.

[270] 付小东，秦建中，腾格尔，等. 固体沥青：反演油气成藏及改造过程的重要标志[J]. 天然气地球科学，2009，20（2）：167-173. [Fu Xiaodong, Qin Jianzhong, Tenger, et al. Solid bitumen: An important sign of inverting the process of hydrocarbon accumulation and reconstruction[J]. Natural Gas Geoscience, 2009, 20(2): 167-173.]

Material Characteristics and Provenance Research of Fine-grained Sedimentary Rocks

Liu XuDong, Peng Jun, Xu TianYu, Wang HaoNan

Natural Gas Geology Key Laboratory of Sichuan Province, School of Earth Science and Technology, Southwest Petroleum University, Chengdu, Sichuan, 610500. China

Abstract: [Significance] The study of the provenance of fine-grained sedimentary rocks is a crucial first step in the "source-to-sink" system theory of fine-grained sedimentary rocks. It is important for restoring the ancient sedimentary environment, understanding the formation mechanism of fine-grained sedimentary rocks, and predicting the distribution of unconventional oil and gas resources. Fine-grained sedimentary rocks are characterized by small particle size, complex composition, and difficulty in observation and research, with different material components corresponding to a variety of sources and origins. A review of the existing research results worldwide shows that currently there is a lack of systematic organization and summary of research outcomes regarding the provenance and origins of fine-grained sedimentary materials.**[Progress]** This paper synthesizes current research findings and categorizes the sources of fine-grained sedimentary rocks into three major types: terrigenous, endogenic, and volcanic-hydrothermal. It provides an in-depth summary and conclusion on the common sources and origins of fine-grained sediments, pointing out: (1) Clay minerals are of detrital weathering origin, diagenetic transformation from other minerals, transformation among clay minerals themselves, hydrolysis of submarine volcanic materials, and biologically mediated by extracellular polymeric substances; (2) Quartz mainly originates from the weathering of terrigenous materials, intra-basin biological activity, devitrification of volcanic ash materials, and authigenic formation; (3) Feldspar originates from the weathering of terrigenous detritus, input from volcanic-hydrothermal activity, and recent studies have also indicated that feldspar can be formed through microbial chemical processes; (4) Carbonate minerals are primarily endogenic, formed through chemical, bio-chemical, biological, and re-transport and deposition processes within the basin, and the input of terrigenous and volcanic-hydrothermal materials not only directly provides carbonate minerals for fine-grained sedimentary rocks but also promotes the formation of carbonate minerals within the basin; (5) Pyrite is mainly formed by the two ore-forming elements, iron and sulfur, through dissimilatory iron reduction and iron shuttling mechanisms, microbial reduction, and thermogenic reduction of sulfate within the basin; (6) Organic matter can be divided into terrigenous vitrinite, inertinite, and some liptinite, as well as endogenic liptinite, zooclastic organic debris, and secondary organic matter. **[Perspectives and conclusions]** Future research on the provenance and origins of fine-grained sedimentary rocks will develop in a multidisciplinary and high-precision direction, and there is still an urgent need for a systematic approach suitable for the study of the provenance of

fine-grained sedimentary rocks.This paper aims to clarify the provenance and origins of fine-grained sedimentary rocks, enhance the understanding of the sources and formation mechanisms of fine-grained sediments, and thus promote the development of fine-grained sedimentology theory. It provides a solid theoretical foundation and scientific basis for identifying the distribution characteristics of fine-grained sedimentary strata and predicting the distribution of unconventional oil and gas resources.

Keywords: fine-grained sedimentary rocks; provenance; material characteristics; mechanism of origin